# 4,6-Diaminopyrimidines as Highly Preferred Troponin I-Interacting Kinase (TNNI3K) Inhibitors
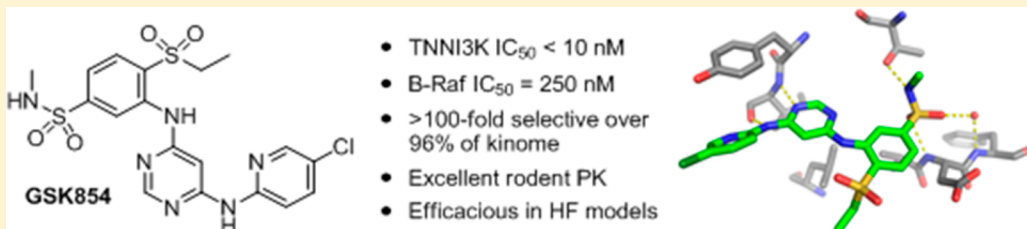
Joanne Philp,[†] Brian G. Lawhorn,*,[†] Alan P. Graves,[‡] Lisa Shewchuk,[‡] Katrina L. Rivera,[†] Larry J. Jolivette,[†] Dennis A. Holt,[†] Gregory J. Gatto, Jr.,[†] and Lara S. Kallander[†]

[†]Heart Failure Discovery Performance Unit and [‡]Platform Technology and Sciences, GlaxoSmithKline, 709 Swedeland Road, King of Prussia, Pennsylvania 19406, United States

**S** *Supporting Information*



- TNNI3K IC$_{50}$ < 10 nM
- B-Raf IC$_{50}$ = 250 nM
- >100-fold selective over 96% of kinome
- Excellent rodent PK
- Efficacious in HF models

GSK854

**ABSTRACT:** Structure-guided progression of a purine-derived series of TNNI3K inhibitors directed design efforts that produced a novel series of 4,6-diaminopyrimidine inhibitors, an emerging kinase binding motif. Herein, we report a detailed understanding of the intrinsic conformational preferences of the scaffold, which impart high specificity for TNNI3K. Further manipulation of the template based on the conformational analysis and additional structure–activity relationship studies provided enhancements in kinase selectivity and pharmacokinetics that furnished an advanced series of potent inhibitors. The optimized compounds (e.g., GSK854) are suitable leads for identifying new cardiac medicines and have been employed as *in vivo* tools in investigational studies aimed at defining the role of TNNI3K within heart failure.

## INTRODUCTION

Troponin I-interacting kinase (TNNI3K) is a self-regulating, cardiac specific kinase that currently lacks a clearly defined biological function.[1,2] Overexpression of *Tnni3k* has been demonstrated to lead to impaired cardiac structure and function in murine models of cardiomyopathy, pressure overload induced heart failure, and in response to acute ischemic injury.[3,4] Conversely, both deletion of *Tnni3k* via transgenic studies and pharmacological inhibition of TNNI3K have been assigned a cardioprotective role within an ischemia/reperfusion setting.[4] Extrapolation of these findings suggests that inhibition of TNNI3K represents a potential novel mechanism for the treatment of heart failure. Accordingly, selective inhibitors of TNNI3K would prove valuable tools in the characterization of the biological role of TNNI3K and provide prospective leads for drug development in an area of continuing unmet medical need.[5,6]

Our efforts to identify potent and selective inhibitors of this promising target uncovered a series of 4,6-diaminopyrimidines that displayed excellent kinase selectivity. Although 2,4-diaminopyrimidines have proven to be a clinically relevant[7,8] and an extensively explored structural class of kinase inhibitors, we noted a much rarer incidence of 4,6-diaminopyrimidines reported in the literature.[9–11] Consideration of the bioactive conformation of the 4,6-diaminopyrimidine template identified the origin of its innate selectivity, and application of these learnings allowed further enhancement of potency, pharmacokinetics, and the kinase selectivity profile of the series.
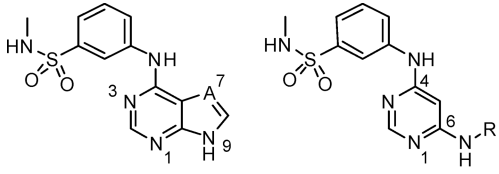
## RESULTS AND DISCUSSION

**Conception and Design of 4,6-Diaminopyrimidines.** As previously disclosed, exploratory screening efforts identified the purine motif, exemplified by compound **1**, as providing potent and tractable TNNI3K inhibitors with promising levels of kinase selectivity.[12] Initial investigation of this scaffold demonstrated that the 7-position nitrogen was not a prerequisite for activity as deazapurine **2** retained potency and selectivity (Table 1).[13] Based on this observation and with the availability of TNNI3K cocrystal structures to direct the design strategy,[12] efforts to identify additional alternatives to the purine core were initiated.

Examination of the crystal structure of **1** bound to TNNI3K highlighted five key hydrogen bond interactions that anchor the molecule within the ATP binding site (Figure 1A). The sulfonamide moiety projects toward the backpocket and contacts TNNI3K via interaction of its NH with Thr539, the "gatekeeper" residue. The sulfonamide oxygens participate in two additional hydrogen bonding interactions, one of which is mediated by a resident water molecule. A bidentate hinge binding interaction was also observed between amino acid Ile542 and the purine core, mediated via the H-bond acceptor capacity of the 3-position nitrogen and the donating ability of the 9-position NH. Notably, in order to simultaneously

**Table 1. Initial Purine and 4,6-Diaminopyrimidine SAR**



| cmpd | A | R | TNNI3K IC$_{50}$ (nM) | % kinases >10-fold selectivity[a] |
|------|-----|---------|------|------|
| 1 | N | - | 500 | 87% (62 of 71) |
| 2 | CH | - | 80 | 94% (61 of 65) |
| 3 | - | 3-Me-Ph | 32 | 96% (69 of 72) |
| 4 | - | 4-CF$_3$–Ph | 79 | 97% (34 of 35) |
| 5 | - | CH$_3$ | 800 | 87% (21 of 24) |

[a]Percent of kinases where off-target kinase IC$_{50}$/TNNI3K IC$_{50}$ > 10.[13]

**Table 2. Initial Modifications of the C6-Aniline**



| cmpd | R | TNNI3K IC$_{50}$ (nM) | % kinases with >10-fold selectivity[a] |
|------|-----|------|------|
| 6 | H | 63 | 95% (36 of 38) |
| 7 | 2-F | 630 | 80% (30 of 38) |
| 8 | 2-Me | 1300 | nd[b] |
| 9 | 2-OMe | 3200 | nd |
| 10 | 3-Cl | 79 | 95% (35 of 37) |
| 3 | 3-Me | 32 | 96% (69 of 72) |
| 11 | 3-OMe | 63 | 92% (34 of 37) |
| 12 | 3-SO$_2$Me | 200 | 88% (22 of 25) |
| 13 | 4-Cl | 79 | 84% (22 of 26) |
| 14 | 4-Me | 79 | 95% (35 of 39) |
| 4 | 4-CF$_3$ | 79 | 97% (34 of 35) |
| 15 | 4-OMe | 160 | 92% (23 of 25) |
| 16 | 4-SO$_2$Me | 79 | 96% (27 of 28) |
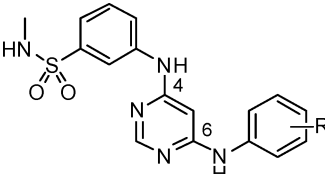
[a]Percent of kinases where off-target kinase IC$_{50}$/TNNI3K IC$_{50}$ > 10.[13]
[b]nd, not determined.

accommodate each of these key H-bond interactions, **1** must adopt a coplanar binding conformation.

In addition to guiding exploration of the deazapurine scaffold[12] study of the crystal structure of **1** led to the conception of 4,6-diaminopyrimidines, such as **3**, which were anticipated to maintain the crucial network of H-bonding interactions of **1** while allowing exploration of the previously unoccupied front pocket from an alternative trajectory. This proved a successful design concept as potency at TNNI3K was improved (16-fold), and critically, the promising kinase selectivity of starting point **1** was upheld with initial 4,6-diaminopyrimidine **3** (Table 1).[13] Indeed, broader evaluation of **3** against a range of kinases indicated an appreciable level of inhibition against only 4% (8 of 189) of kinases when tested at 1 μM inhibitor concentration in the Millipore KinaseProfiler panel (see Supporting Information). A cocrystal structure of **4**, a close analog of **3**, bound to TNNI3K confirmed that the intricate H-bond mediated recognition pattern of **1** and consequent coplanar configuration were maintained (Figure 1B). The critical binding contribution of the aromatic ring of the C6 aniline in the front pocket is highlighted by the fact that truncated analog **5** displays over an order of magnitude reduction in TNNI3K affinity, perhaps indicating a benefit imparted by space filling or the influence of conformational preferences, or a combination of both of these factors.

Following the encouraging data observed with **3**, an exploration of alternative C6 substituents was initiated, and evidence of a tractable structure−activity relationship (SAR) against TNNI3K readily emerged (Table 2), with a clear indication of a steric driven intolerance to substitution at the C2 ring position, reflected in the reduced activity observed with

analogs **7**−**9**. In contrast, incorporation of a variety of functional groups at both the meta and para positions was permitted by the target. At these positions, electron withdrawing (**10**, **12**, **13**, **4**, and **16**) and electron donating (**3**, **11**, **14**, and **15**) groups of differing sizes could be accommodated. Favorable kinase selectivity[13] was maintained across this range of analogs, which encouraged us to further investigate the series and the underlying origins of its specificity for TNNI3K.

**General Kinase Selectivity.** To decipher the features of **3** that contribute to its unique affinity and selectivity for TNNI3K, a series of heterocyclic core analogs were evaluated. Replacement of the pyrimidine N3 atom with CH to give pyridine **17** resulted in a substantially less effective inhibitor (>100-fold) of TNNI3K, illustrating a critical role for the N3 nitrogen (Figure 2). In some instances where 4,6-diaminopyrimidines exhibit preferential binding to a kinase, N3 has been observed to participate in a specific interaction that facilitates binding and imparts significant overall kinase selectivity.[10] However, the cocrystal structure of **4** did not indicate an interaction of this nature; instead, this dramatic effect was attributed to the introduction of a potential severe steric interaction (~3 kcal/mol for planar vs skewed conformation for related diphenylamines)[14c] between the pyridine C5−H and
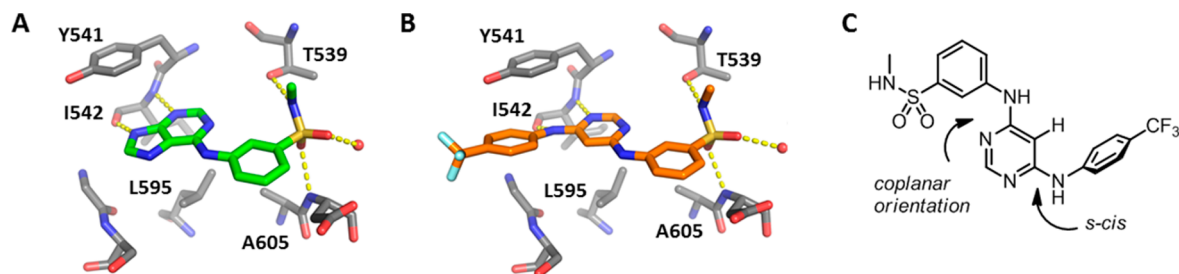


**Figure 1.** Cocrystal structures of **1** (A, PDB 4YFI)[12] and **4** (B, PDB 6B5J) bound to TNNI3K and (C) a 2D representation of the binding mode of **4**.
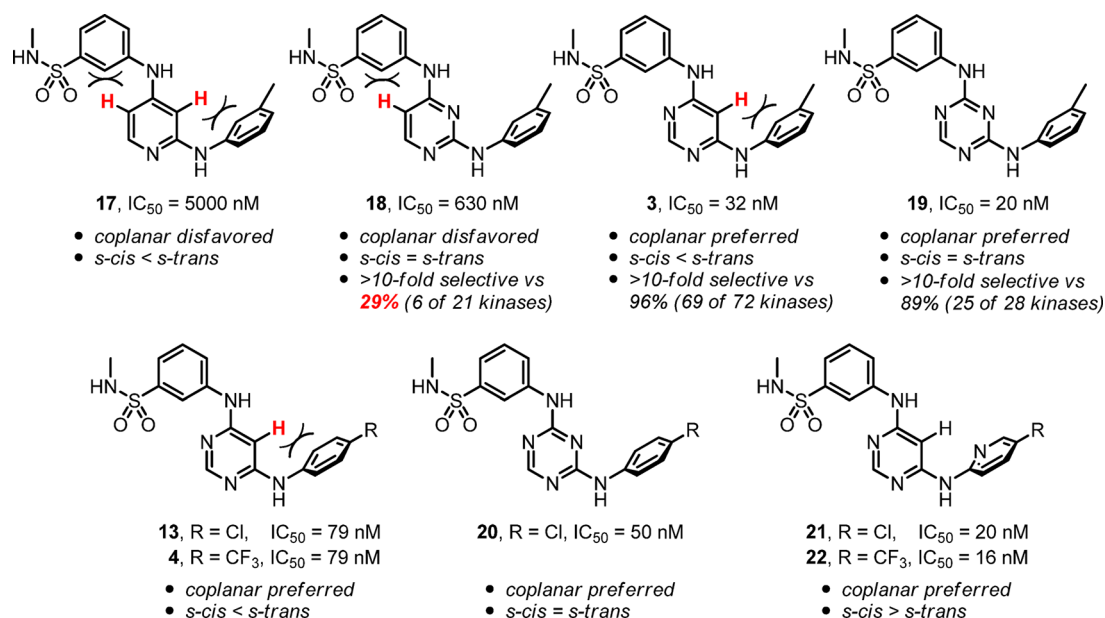
**Figure 2.** Two-dimensional representation of the preferred TNNI3K binding mode for various heterocyclic cores.

the benzenesulfonamide C2−H (Figure 2). As a consequence, pyridine **17** is unable to adhere to the highly preferred coplanar binding conformation (Figure 1) that is adopted by **3** leading to reduced activity. Similarly, it is proposed that compound **18**, the 2,4-diaminopyrimidine counterpart of **3**, exhibits a reduced potency arising from this conformational bias (Figure 2). However, this pyrimidine exhibits a heightened (∼8-fold) affinity for TNNI3K compared to pyridine **17**, in line with the greater capacity of **18** to conform to the s-cis orientation required for optimal hinge binding (Figure 1).[10,14] Specifically, the N3 of **18** alleviates the steric interaction (∼2 kcal/mol for s-cis vs s-trans for related anilinopyrimidines)[14b] between the C3−H of pyridine **17** and the C6 aryl resulting in an improved bidentate hinge binding interaction with TNNI3K. In fact, the reduced inhibition of TNNI3K observed for 2,4-diaminopyrimidine **18** compared to 4,6-diaminopyrimdine **3** represents a departure from the norm, as most kinases prefer 2,4-diaminopyrimidines because of this innate ability to adopt the s-cis configuration.[9,10,15] As a result, in contrast to **3**, 2,4-diaminopyrimidine **18** is a promiscuous kinase inhibitor that exhibits substantial activity against many (15/21) of the kinases examined.[10] These observations also explain the reduction of TNNI3K affinity associated with ortho-substituted C6 aryls (Table 2, **7**−**9**) wherein the preferred s-cis configuration is further compromised. Incorporating these SAR and structure informed conformational considerations into compound design led to preparation of triazine **19**, which simultaneously relieves the steric penalties observed in the 2,4- and 4,6-diaminopyrimdine frameworks upon enzyme binding. Consequently, **19** exhibits comparable or increased affinity over **3** (1.6-fold) and **18** (32-fold), and the kinase selectivity associated with these conformational preferences is restored (Figure 2).[13]

An alternative but equally effective approach to favor the optimal TNNI3K binding mode within the 4,6-diaminopyrimidine system was realized in the design of compounds **21** and **22** (Figure 2), which incorporates a 2-pyridyl substituent in place of the C6 aniline of **3**. Inclusion of the pyridyl nitrogen reinforces the requisite s-cis conformation by removing the steric interaction with C5−H of the pyrimidine and
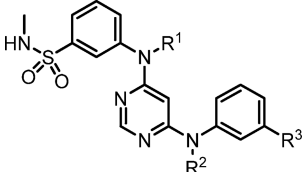
simultaneously serves to destabilize the alternative s-trans orientation by introducing a lone pair−lone pair repulsion.[14b] As such, enhanced potency (2.5-fold) is achieved within pyridyl pyrimidine analog **21** compared to the analogous phenyl triazine **20**. Comparison of the potency of the phenyl vs 2-pyridyl analog pairs **13**/**21** and **4**/**22** confirms the conformational hypothesis and defines the magnitude (∼4−5-fold) of the conformational bias and resultant enhanced hinge binding capacity imparted by the pyridyl nitrogen. Independent of our efforts, an analogous 2-pyridyl unit has been employed in the design of Lck inhibitors based on a similar conformational rationale.[14b] However, as direct phenyl analogs of the 2-pyridyl substituents were not reported in that study, the experiments disclosed herein confirm the value of the 2-pyridyl design, provide the magnitude of the effect experimentally (0.8 kcal/mol using $\Delta G_1 - \Delta G_2 = RT \ln(K_1/K_2)$ where $K$ is approximated by IC$_{50}$ values of **13** and **21** or **4** and **22**), and distinguish the contribution of the pyridyl N toward stabilizing the s-cis conformation from other binding benefits arising from the incorporation of C6-aryl amines (e.g., **3**, IC$_{50}$ = 32 nM) instead of C6-alkyl amines (e.g., **5**, IC$_{50}$ = 800 nM). As anticipated, pyridines **21** and **22** maintain the good overall kinase selectivity profile of the parent system (>10-fold selectivity vs >90% of kinases tested)[13] and represent optimal leads for further development.

Overall, the TNNI3K selectivity of 4,6-diaminopyrimidines (e.g., **3**) can be primarily attributed to their unique ability to adopt a coplanar binding conformation (Figure 2). This allows the compounds to engage the hinge region H-bond interactions while simultaneously positioning the sulfonamide to hydrogen bond with the gatekeeper threonine (unique to 19% of the kinome) and form polar contacts within the backpocket (Figure 1). As within other reports of favored binding by 4,6-diaminopyrimidines the N3 nitrogen has a pivotal role in the attainment of this preferential binding, and as such the 4,6-diaminopyrimdine scaffold may be considered a privileged structure for obtaining selectivity against the kinome.[10,14b]

**EGFR Selectivity.** Although parent compound **3** generally demonstrated an excellent kinase selectivity profile, a potential

liability for the series is its potent inhibition of epidermal growth factor receptor (EGFR) kinase. Although a valid antioncogenic target, inhibition of EGFR has been associated with cardiac dysfunction.[16] The presence of such an off-target activity would also confound interpretation of target validation studies for TNNI3K. Therefore, it was deemed necessary to attenuate this off-target activity to progress the 4,6-diaminopyrimdines. This undesired activity is consistent with findings that a related 4,6-diaminopyrimidine template can bind preferentially to EGFR.[10a] Encouragingly, initial SAR efforts demonstrated that replacement of the 3-methyl substituent of **3** with a larger group such as the isopropyl of **23** (Table 3)

### Table 3. Optimization of Selectivity for TNNI3K vs EGFR



| cmpd | $R^1$ | $R^2$ | $R^3$ | TNNI3K IC$_{50}$ (nM) | EGFR IC$_{50}$ (nM) | selectivity (fold)[a] |
|------|-------|-------|-------|------------------------|----------------------|------------------------|
| 3 | H | H | Me | 32 | 3 | 0.1 |
| 23 | H | H | $i$-Pr | 50 | 25 | 0.5 |
| 24 | H | H | $t$-Bu | 400 | 400 | 1 |
| 25 | H | H | SO$_2$NHMe | 79 | 1600 | 20 |
| 26 | H | H | NO$_2$ | nd[b,c] | 4 | nd |
| 27 | H | Me | Me | 2000 | 20 | 0.01 |
| 28 | Me | H | Me | 8000 | 2000 | 0.25 |

[a]Selectivity = EGFR IC$_{50}$/TNNI3K IC$_{50}$. [b]nd, not determined. [c]Cmpd **26** showed modest activity (IC$_{50}$ = 500 nM) in a TNNI3K cellular assay.

resulted in a 7-fold reduction of EGFR inhibition with minimal impact on TNNI3K affinity. Further increasing the steric demand of this substituent, as highlighted by $t$-butyl analog **24**, provided an inhibitor that was equipotent at TNNI3K and EGFR. Bis-sulphonamide compound **25** represented a key advance, as it led to an inversion of TNNI3K-EGFR preference compared to parent compound **3**. SAR indicated that this selectivity gain was not governed by electronics given that analog **26**, containing the strongly electron withdrawing nitro group, displayed comparable EGFR inhibition to **3**. To fully interpret this steric-driven effect on EGFR activity, compound **3** was docked into a crystal structure (PDB 4I23) of EGFR (Figure 3). Although both enzymes contain a threonine gatekeeper, EGFR has a smaller back pocket than TNNI3K

as a result of two point changes between the active sites (Ala605 to Thr854 and Leu513 to Met766). Thus, it is hypothesized that there is insufficient space within EGFR to tolerate the sulfonamide projecting into its back pocket. These observations suggest that within EGFR the 4,6-diaminopyrimidines reside in a flipped binding mode wherein the smaller C6-aniline group occupies the back pocket (Figure 3). In this binding proposal, which mirrors that put forward by Gray for related 4,6-diaminopyrimidine EGFR inhibitors, the pyrimidine N1 participates in a hydrogen bond with the gatekeeper Thr790 leading to its uniquely potent activity at EGFR.[10]

Further evidence for this alternative binding mode is exemplified by the relative insensitivity of EGFR activity to the methylation of the C6 linked NH (**27**, Table 3). In contrast, TNNI3K activity is vastly reduced by the removal of this hinge binding NH. Conversely, alkylation of the C4 NH (**28**), which represents the hinge binding NH within EGFR, results in serious attenuation of activity at this kinase. Interestingly, this methylation is also detrimental to TNNI3K affinity because **28** is prevented from assuming the crucial coplanar binding conformation as this would introduce at least one severe H/H overlapping interaction between the N-Me and its neighboring aryl hydrogens.[12]

As a consequence of this alternative binding mode in EGFR, divergent SAR is also observed with C6-phenyl analog **13** (EGFR IC$_{50}$ = 13 nM) and its C6-pyridyl derivative **21** (EGFR IC$_{50}$ = 630 nM, Figure 2), indicating the pyridyl nitrogen is not well tolerated in the lipophilic back pocket of EGFR. As a result, **21** exhibits significant selectivity (32-fold) for TNNI3K over EGFR.

**Pharmacokinetic Properties.** The initial 4,6-diaminopyrimidine inhibitor **3** showed a poor pharmacokinetic profile with high clearance and low oral bioavailability in the rat (Table 4). To reduce the metabolic liability of **3**, the 3-methyl group was replaced with a halogen to give analogs **10** and **29**, which offered a modest improvement in clearance. Relocating the halogen substituent to the 4-position of the C6 aryl proved beneficial with analog **13** providing a further 2-fold reduction in clearance versus **10** and **29**. These results suggest oxidation of the aniline ring may be a primary metabolic pathway for **3** that can be blocked through appropriate substitution. Compound **13** also offered enhanced oral bioavailability over **3**, which may result from reduced first-pass clearance. Importantly, TNNI3K inhibitor **21**, which had been optimized for potency by inclusion of the 2-pyridyl moiety, maintained the attractive PK profile of its phenyl analog **13**, indicating the 4-Cl-2-pyridyl aniline is an optimal C6-moiety.
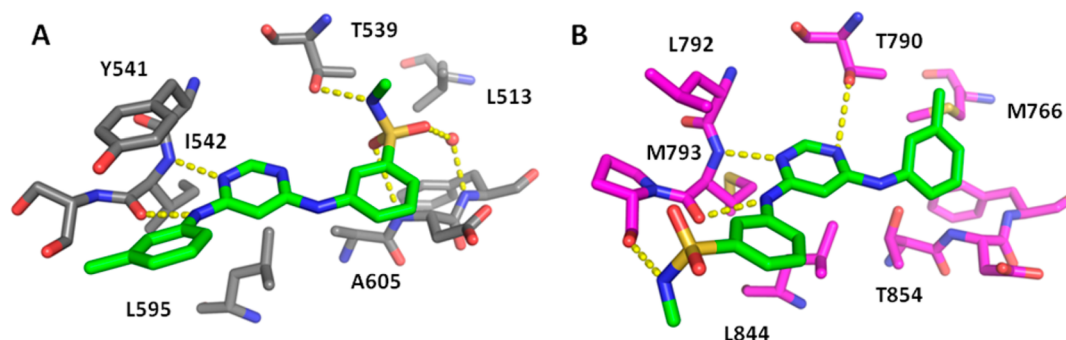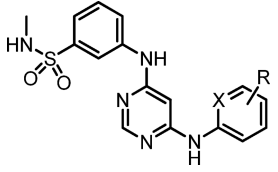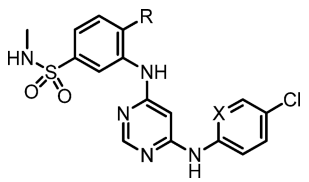


**Figure 3.** Model of **3** bound to TNNI3K (A, PDB 6B5J) and EGFR (B, PDB 4I23).

## Table 4. Pharmacokinetics of Initial 4,6-Diaminopyrimidines



| cmpd | X | R | rat Cl (mL/min/kg) | rat PO DNAUC (h·kg/L) | oral F (%) | TNNI3K IC$_{50}$ (nM) |
|---|---|---|---|---|---|---|
| 3 | CH | 3-Me | 86 | 0.037 | 19 | 32 |
| 10 | CH | 3-Cl | 52 | 0.064 | 20 | 79 |
| 29 | CH | 3-Br | 53 | 0.10 | 33 | 79 |
| 13 | CH | 4-Cl | 23 | 0.71 | 100 | 79 |
| 21 | N | 4-Cl | 16 | 0.67 | 65 | 20 |

## Table 5. Optimization of the C4-Substituent



| cmpd | X | R | rat Cl (mL/min/kg) | rat PO DNAUC (h·kg/L) | oral F (%) | TNNI3K IC$_{50}$ (nM) |
|---|---|---|---|---|---|---|
| 13 | CH | H | 25 | 0.71 | 100 | 79 |
| 30 | CH | F | nd[a] | 1.1 | nd | 200 |
| 31 | CH | Cl | 14 | 0.70 | 55 | 130 |
| 32 | CH | Me | nd | nd | nd | 160 |
| 33 | CH | OMe | 26 | 0.69 | 100 | 50 |
| 34 | CH | SMe | 4.5 | 2.1 | 52 | 400 |
| 35 | CH | NHMe | nd | nd | nd | 2500 |
| 36 | CH | NMe$_2$ | 52 | 0.096 | 30 | 79 |
| 37 | N | OMe | 9.9 | 1.3 | 75 | ≤10[b] |
| 38 | CH | OCF$_3$ | 16 | 0.86 | 84 | 32 |
| 39 | N | OCF$_3$ | 12 | 0.91 | 67 | nd[c] |
| 40 | CH | OCH$_2$CF$_3$ | 20 | 0.32 | 37 | 25 |
| 41 | N | OCH$_2$CF$_3$ | 7.4 | 2.3 | 99 | ≤10 |

[a]nd, not determined. [b]Compound IC$_{50}$ values less than 10 nM could not be accurately obtained due to titration of TNNI3K in the enzyme assay. [c]Cmpd 39 showed enhanced activity (IC$_{50}$ = 63 nM) over 38 (IC$_{50}$ = 320 nM) in a TNNI3K cellular assay.

Next, we turned our attention to exploiting other positions within the molecule to further enhance the inhibitory activity and PK profile of the series. Based on the X-ray crystal structure of 4 bound to TNNI3K (Figure 1), we selected to probe the C4 position of the benzenesulfonamide, as C4-substituents were expected to project favorably into a relatively open area within the TNNI3K binding pocket. The initial analogs (30−36, Table 5) indicated that substitutions at the C4 position greatly influenced TNNI3K activity, but modeling of the substituents in the TNNI3K active site revealed that steric effects could not account for the observed SAR. In our recent publication, the varying effects of these C4-substituents on TNNI3K binding were rationalized based on three separate phenomena: (1) electronic modulation of the sulfonamide H-bond donor interaction with TNNI3K (cf. 31, 35), (2) intramolecular hydrogen bonding between C4-substituents and the neighboring aniline NH (cf. 32, 33), and (3) stereo-electronic effects of mono- versus disubstituted ortho-anilines (cf. 35, 36).[17] As a result of these effects, highly electron donating substituents exhibit poor potency (e.g., 35) by disrupting hydrogen bonding between the inhibitor and TNNI3K, whereas groups that lack an ability to form an internal hydrogen bond with the ortho-aniline NH are also

moderately potent (e.g., 30, 31, 32, 34). However, the mildly electron donating MeO substituent (33), which can engage in an internal H-bond with the ortho-aniline NH, exhibited good TNNI3K activity (IC$_{50}$ = 50 nM) and retained the favorable PK properties of the unsubstituted parent 13.

This result prompted a survey of additional C4-ether analogs (37−41), which revealed that compounds bearing ethers with reduced electron-donating ability (e.g., 40−41) or electron-withdrawing ability (e.g., 38-39) displayed enhanced activity at TNNI3K while maintaining excellent PK properties. These results also served to further verify the value of the C6 aryl pyridyl nitrogen as this modification consistently provided elevated inhibitory activity against TNNI3K in conjunction with reduced clearance across each of the matched pairs (Table 5; 33/37, 38/39 and 40/41).

While optimizing the pharmacokinetic properties of the TNNI3K inhibitors, we found TPSA to be an important determinant of oral bioavailability in the series (Figure 4) as compounds exhibiting TPSA ≥ 123 Å$^2$ were consistently observed to show low oral exposure (F < 30% for 28 of 28 tested) in rats. By contrast, compounds with TPSA < 123 Å$^2$ showed a reasonable likelihood for high oral bioavailability (F > 30% for 69 of 128 tested), and those compounds displaying
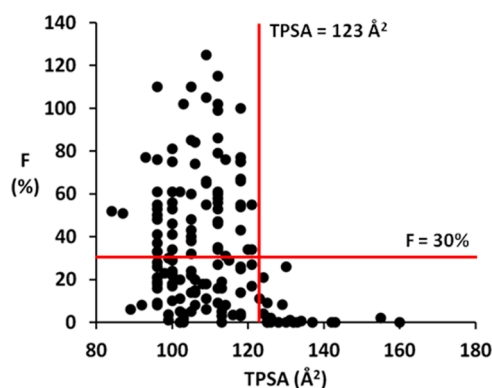
**Figure 4.** Plot of oral bioavailability (*F*) vs TPSA for benzenesulfonamide TNNI3K inhibitors.



**Figure 5.** Models of **37** in TNNI3K (A, PDB 6B5J) and B-Raf (B, PDB 4YHT) and **43** in TNNI3K (C, PDB 6B5J) and B-Raf (D, PDB 4YHT).

poor oral exposure within this class typically exhibited very low aqueous solubility or contained a charged functional group, which may negatively impact their passive permeability. This finding is consistent with the historical use of TPSA and $PSA_d$ in drug design, and it is noteworthy that TPSA was found to be a superior predictor of oral bioavailability within this series when compared to any other calculated property (e.g., cLogP, %PSA, HBA, HBD), measured property (e.g., artificial membrane permeability, ChromLogD), or a multiparameter permeability model.[18] This highlights the remarkable ability of the simple TPSA calculation to capture the physical processes (e.g., desolvation) involved in passive membrane permeability and its utility for guiding lead optimization when competing effects (e.g., internal H-bonds, varying charge states) do not obscure its predictive relationship with oral bioavailability.[18]

**B-Raf Selectivity.** The 4,6-diaminopyrimidine **37** is a highly potent analog that showed promising PK and notably also maintains the broad spectrum kinase selectivity of the series, with >50-fold selectivity against 27 of 29 (93%) kinases assessed. However, **37** displays potent activity against B-Raf (IC$_{50}$ = 20 nM), a kinase that shares 82% sequence similarity with TNNI3K among its ATP-binding site residues, and elimination of this activity was considered critical since inhibition of Raf kinases has been linked to effects in heart failure models.[19] A comparison of **37** modeled into X-ray crystal structures of TNNI3K and B-Raf (Figure 5) reveals a key residue difference between the two kinase active sites. In TNNI3K, Leu595 resides below the 4,6-diaminopyrimidine inhibitor, whereas B-Raf contains Phe582 in the corresponding position. We have previously introduced selectivity for TNNI3K over B-Raf by exploiting the electrostatic differences between these two residues in a related series of TNNI3K inhibitors.[17,20] To optimize the 4,6-diaminopyrimidine inhibitors we sought a complementary approach that would introduce selectivity for TNNI3K based on the observed steric differences between TNNI3K and B-Raf. We noted the proximity of the 4-OMe group of **37** to Leu595 of TNNI3K and the Phe582 residue of B-Raf (Figure 5) and hypothesized that larger 4-substituents might be accommodated by TNNI3K while introducing a steric clash with the larger B-Raf Phe582 residue. Additional residues near the 4-OMe group of **37** are conserved between TNNI3K (Gly470, Ser471, Asn593) and B-Raf (Gly463, Ser464, Asn580), but Ser464 in B-Raf occupies an alternate position relative to Ser471 in TNNI3K that further constrains the size of the B-Raf pocket relative to TNNI3K (Figure 5).
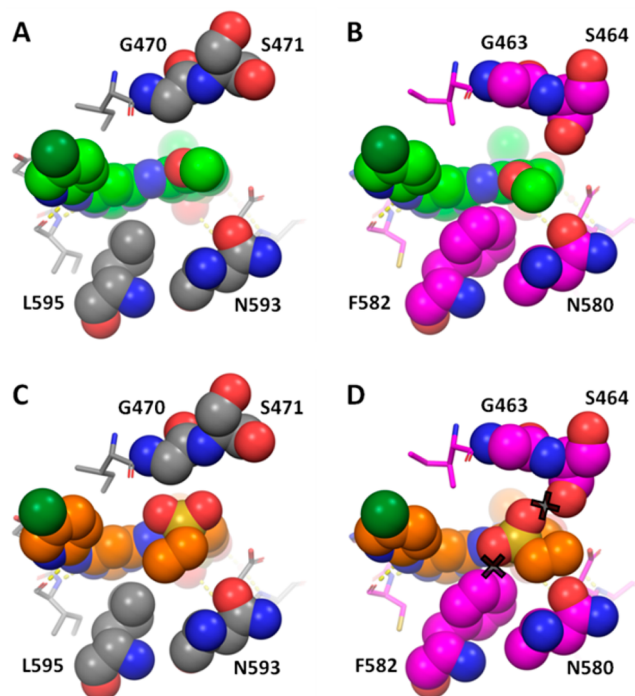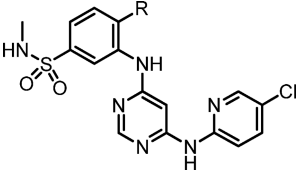
Larger 4-substituents that remain in the plane of the aryl ring did not impart selectivity as compounds such as **41** exhibited potent B-Raf activity (IC$_{50}$ = 13 nM). Thus, we synthesized and evaluated a series of 4-sulfonyl analogs (Table 6) of varying sizes, anticipating that these groups would project out of the plane of the aryl rings and project toward Leu595 and Ser471 of TNNI3K and clash with Phe582 and Ser464 of B-Raf (Figure 5). Other critical features of the sulfone moiety that pointed to its selection as an ideal 4-substituent included its electron-withdrawing nature and ability to form an internal H-bond with the neighboring aniline NH, both of which are required for optimal TNNI3K binding (*vide supra*).[17,21] An initial methyl sulfone analog **42** retained good potency at TNNI3K and high oral exposure in rats while reducing B-Raf activity by 10-fold. Expanding the size of the sulfonyl group further attenuated B-Raf binding in a stepwise fashion (**43**−**45**) with no detrimental impact on TNNI3K affinity, such that the *tert*-butyl sulfone (**45**) exhibited ≥200-fold selectivity for TNNI3K over B-Raf. This significant size-dependent enhancement in selectivity corroborates our model showing that TNNI3K contains a larger pocket in this region compared to B-Raf (Figure 5). In addition, the model of **43** bound to B-Raf suggests that one of its sulfonyl oxygens is in close contact with the backbone carbonyl of Ser464, likely creating an electrostatic repulsion that further contributes to the loss in potency for B-Raf. The oral exposure of the *i*-Pr (**44**) and *t*-Bu (**45**) analogs was reduced compared to **42**, and therefore, the ethyl sulfone **43** was deemed to have the optimal balance of selectivity and PK properties for use as an *in vivo* tool in heart failure models.

Compound **43** (GSK854)[4] exhibits substantial selectivity against B-Raf (>25-fold) and EGFR (IC$_{50}$ > 25 μM), excellent broad spectrum kinase selectivity with >100-fold selectivity over 96% of kinases tested (≤50% inhibition @ 1 μM for 282 of 294 kinases, see Supporting Information), high activity in a

## Table 6. 4-Sulfonylbenzenesulfonamide SAR



| cmpd | R | TNNI3K IC$_{50}$ (nM) | B-Raf IC$_{50}$ (nM)[a] | selectivity (fold)[b] | rat PO DNAUC (h·kg/L) |
|------|------|------|------|------|------|
| 37 | OMe | ≤10[c] | 20 | ≥2 | 1.3 |
| 42 | SO$_2$Me | 13 | 200 | 15 | 0.76 |
| 43 | SO$_2$Et | ≤10 | 250 | ≥25 | 0.56 |
| 44 | SO$_2$iPr | ≤10 | 500 | ≥50 | 0.27 |
| 45 | SO$_2$tBu | ≤10 | 2000 | ≥200 | 0.076 |

[a]Raf activity was evaluated using the B-Raf (V600E) mutant kinase. [b]Selectivity = B-Raf IC$_{50}$/TNNI3K IC$_{50}$. [c]Compound IC$_{50}$ values less than 10 nM could not be accurately obtained due to titration of TNNI3K in the enzyme assay.

### Scheme 1
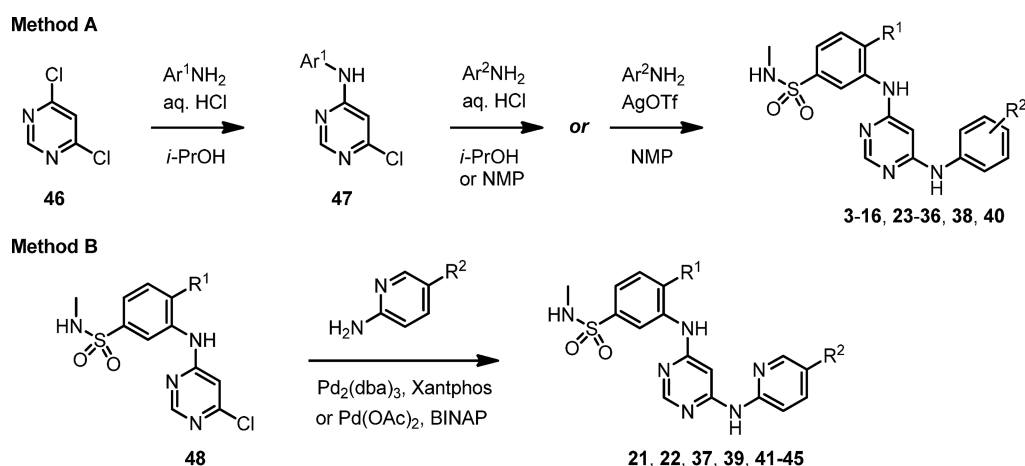


TNNI3K cellular assay (IC$_{50}$ = 8 nM), good pharmacokinetics in rats (Cl = 14 mL/min/kg, Vdss = 1.9 L/kg, $t_{1/2}$ = 2.3 h, F = 48%), and useful exposures in mice (100 mg/kg/d dietary dose gives blood concentration = 0.4−1.6 µM total, 14−56 nM free and heart concentration = 1.1 µM total, mouse PPB F$_u$ = 3.5%) and thus has been employed in rodent models and cellular assays to delineate the cardiac biology of TNNI3K.[4] Notably, mice treated with **43** for 6 weeks following a myocardial infarction exhibited reduced left ventricular dysfunction and remodeling compared to vehicle controls, and these effects were linked to reduced ROS and reduced p38 MAP kinase activation.[4]

### ■ CHEMISTRY

4,6-Diaminopyrimidine TNNI3K inhibitors were synthesized through sequential, acid-mediated (HCl or AgOTf) substitutions[10,11,17] of 4,6-dichloropyrimidine (**46**) with appropriately adorned anilines (Scheme 1, Method A), which were either commercially available or synthesized as described previously.[12,22] Typically, microwave irradiation was employed to accelerate reaction rates on small scale, while conventional heating conditions were used for multigram preparations.[23] Pyridine (**17**), 2,4-diaminopyrimidine (**18**), and triazine (**19**, **20**) variants were synthesized in an analogous fashion from 2,4-dichloropyridine, 2,4-dichloropyrimidine, or 2,4,6-trichloro-1,3,5-triazine, respectively. Incorporation of 2-aminopyridine substituents was accomplished through Pd-catalyzed cross

coupling with the monochloride intermediate **48** (Scheme 1, Method B).[10,11]

### ■ CONCLUSIONS

Structure-based design led to the discovery of a series of 4,6-diaminopyrimidines that function as highly specific TNNI3K inhibitors that are valuable probes for understanding the biology of TNNI3K. Further scrutiny of the binding mode of these 4,6-diaminopyrimidines and the SAR of alternative heterocycles demonstrated that the 4,6-diaminopyrimidine scaffold uniquely produces potent and selective inhibitors as a result of its intrinsic conformational preferences. Application of this analysis to analog design produced further enhancements in TNNI3K affinity. Concurrent interpretation of additional SAR uncovered simple and predictable strategies to weaken activity at EGFR and B-Raf, two homologous kinases for which the 4,6-diaminopyrimidines also serve as a privileged structure, albeit by virtue of a variant mechanism and binding mode for EGFR. The pharmacokinetics of the 4,6-diaminopyrimidines was also optimized, which culminated in the discovery of **43**, a preferred TNNI3K inhibitor tool compound and lead for discovery of new medicines.

### ■ EXPERIMENTAL SECTION

**General Experimental.** Compounds were evaluated for activity against TNNI3K and B-Raf (V600E) as previously described.[12] For the TNNI3K enzyme assay, compound IC$_{50}$ values less than 10 nM could not be accurately obtained due to titration of TNNI3K in the

assay. TNNI3K cellular assays, rat pharmacokinetics, and X-ray crystallography studies were conducted as previously described.[12] All studies were conducted in accordance with the GSK Policy on the Care, Welfare, and Treatment of Laboratory Animals and were reviewed by the Institutional Animal Care and Use Committee either at GSK or by the ethical review process at the institution where the work was performed. The purity of each inhibitor was determined to be >95% on an Agilent 1100 HPLC equipped with a Sunfire C18 5.0 $\mu$m column (3.0 mm × 50 mm) using a gradient of 10% to 100% MeCN/$H_2O$/0.05% TFA at 1 mL/min flow rate with detection at 220 and 254 nm. Mass determinations were conducted using an Agilent 6110 Quadrupole MS with positive ESI. Preparative HPLC was conducted on a Waters 2525 system at a flow rate of 50 mL/min with 254 nm detection using either a Sunfire C18 OBD 5 $\mu$m column (30 × 150 mm) with a gradient of MeCN/$H_2O$/0.1% TFA or an Xbridge C18 OBD 5 $\mu$m column (30 × 150 mm) with a gradient of MeCN/aq $NH_4OH$ pH 10. Flash column chromatography was conducted on silica gel eluting with EtOAc−hexanes or MeOH−$CH_2Cl_2$ mixtures or with a sequence of $CH_2Cl_2$, $Et_2O$, EtOAc, and acetone. Compounds were synthesized using procedures that followed reported protocols,[17,22] and specific experimental details have been published previously for compounds **1**, **2**, **13**, **30−36**, **38**, and **40**.[12,17] Reagents and building blocks were purchased and used as is or synthesized following reported procedures.[12,22]

*Method A. General Coupling Method for Anilines and Chloropyrimidines.* A mixture of a chloro-heterocycle and the required aniline (1.3 equiv) in *i*-PrOH or NMP (2 mL) was treated with 1 M aqueous HCl (1 equiv) and subjected to microwave irradiation (150 °C) for 15−60 min before being cooled to room temperature. Analytically pure solids were obtained after purification by reverse-phase HPLC (**4**, **6**, **7**, **8**, **10**, **11**, **12**, **16**, **23**, **24**, **25**, **26**, **27**, and **28**), flash column chromatography (**3** and **9**), or by collecting the precipitate by filtration (**5**, **14**, and **15**).

*Method B. General Coupling Method for 2-Aminopyridines and Chloro-pyrimidines.* A mixture of a chloro-heterocycle, the required aniline (1.3 equiv), Pd$_2$(dba)$_3$ (0.02 equiv), Xantphos (0.04 equiv), and K$_3$PO$_4$ in 1,4-dioxane (1.3 mL) was subjected to microwave irradiation (150 °C) for 30−90 min before being cooled to room temperature. Analytically pure solids were obtained after purification by reverse-phase HPLC (**21**, **22**, **37**, **39**, **41**, **42**, **44**, and **45**).

*N-Methyl-3-({6-[(3-methylphenyl)amino]-4-pyrimidinyl}amino)-benzenesulfonamide Trifluoroacetate (3).* Compound **3** was prepared from 6-chloro-*N*-(3-methylphenyl)-4-pyrimidinamine and 3-amino-*N*-methylbenzenesulfonamide using Method A as a cream solid in 15% yield (89 mg): $^1$H NMR (400 MHz, DMSO-$d_6$) $\delta$ 9.75 (s, 1H), 9.43 (br. s., 1H), 8.37 (s, 1H), 8.02−8.11 (m, 1H), 7.87 (dd, $J$ = 1.51, 8.03 Hz, 1H), 7.54 (t, $J$ = 7.91 Hz, 1H), 7.46 (q, $J$ = 4.85 Hz, 1H), 7.38 (d, $J$ = 7.78 Hz, 1H), 7.29−7.35 (m, 2H), 7.20−7.27 (m, 1H), 6.90 (d, $J$ = 7.28 Hz, 1H), 6.18 (s, 1H), 2.44 (d, $J$ = 4.77 Hz, 3H), 2.31 (s, 3H). MS ($m/z$) 370.1 (M + H$^+$).

*N-Methyl-3-[(6-{[4-(trifluoromethyl)phenyl]amino}-4-pyrimidinyl)amino]benzenesulfonamide Trifluoroacetate (4).* Compound **4** was prepared from 3-[(6-chloro-4-pyrimidinyl)amino]-*N*-methylbenzene-sulfonamide and 4-(trifluoromethyl)aniline using Method A as a white solid in 21% yield (52 mg): $^1$H NMR (400 MHz, DMSO-$d_6$) $\delta$ 9.71 (s, 1H), 9.67 (s, 1H), 8.42 (s, 1H), 8.11 (t, $J$ = 1.88 Hz, 1H), 7.93 (dd, $J$ = 1.51, 8.28 Hz, 1H), 7.86 (d, $J$ = 8.78 Hz, 2H), 7.65 (d, $J$ = 8.78 Hz, 2H), 7.53 (t, $J$ = 8.03 Hz, 1H), 7.45 (q, $J$ = 5.02 Hz, 1H), 7.35 (d, $J$ = 7.78 Hz, 1H), 6.27 (s, 1H), 2.45 (d, $J$ = 5.02 Hz, 3H). MS ($m/z$) 423.9 (M + H$^+$).

*N-Methyl-3-{[6-(methylamino)-4-pyrimidinyl]amino}-benzenesulfonamide Hydrochloride (5).* Compound **5** was prepared from 6-chloro-*N*-methyl-4-pyrimidinamine and 3-amino-*N*-methylbenzenesulfonamide using Method A as a white solid in 57% yield (106 mg): $^1$H NMR (400 MHz, DMSO-$d_6$) $\delta$ 10.61 (br. s., 1H), 8.82 (br. s., 1H), 8.44 (s, 1H), 7.95 (br. s., 1H), 7.75 (br. s., 1H), 7.55−7.67 (m, 2H), 7.52 (d, $J$ = 7.28 Hz, 1H), 6.08 (br. s., 1H), 2.88 (br. s., 3H), 2.45 (d, $J$ = 4.77 Hz, 3H). MS ($m/z$) 294.0 (M + H$^+$).

*N-Methyl-3-{[6-(phenylamino)-4-pyrimidinyl]amino}-benzenesulfonamide Trifluoroacetate (6).* Compound **6** was prepared from 3-[(6-chloro-4-pyrimidinyl)amino]-*N*-methylbenzene-sulfonamide and aniline using Method A as a white solid in 35% yield (84 mg): $^1$H NMR (400 MHz, DMSO-$d_6$) $\delta$ 9.75 (br. s., 1H), 9.49 (br. s., 1H), 8.38 (s, 1H), 8.07 (br. s., 1H), 7.87 (d, $J$ = 8.03 Hz, 1H), 7.53 (d, $J$ = 6.78 Hz, 3H), 7.46 (d, $J$ = 4.27 Hz, 1H), 7.29−7.41 (m, 3H), 7.02−7.16 (m, 1H), 6.99 (s, 1H), 6.20 (s, 1H), 2.44 (d, $J$ = 4.27 Hz, 3H). MS ($m/z$) 356.0 (M + H$^+$).

*3-({6-[(2-Fluorophenyl)amino]-4-pyrimidinyl}amino)-N-methyl-benzenesulfonamide Trifluoroacetate (7).* Compound **7** was prepared from 3-[(6-chloro-4-pyrimidinyl)amino]-*N*-methylbenzene-sulfonamide and 2-fluoroaniline using Method A as a yellow solid in 26% yield (33 mg): $^1$H NMR (400 MHz, DMSO-$d_6$) $\delta$ 9.71 (s, 1H), 9.21 (s, 1H), 8.33 (s, 1H), 8.08 (s, 1H), 7.83−7.89 (m, 1H), 7.71−7.78 (m, 1H), 7.49−7.56 (m, 1H), 7.45 (q, $J$ = 4.85 Hz, 1H), 7.36 (d, $J$ = 7.78 Hz, 1H), 7.27−7.34 (m, 1H), 7.17−7.25 (m, 2H), 6.12 (s, 1H), 2.44 (d, $J$ = 5.02 Hz, 3H). MS ($m/z$) 374.1 (M + H$^+$).

*N-Methyl-3-({6-[(2-methylphenyl)amino]-4-pyrimidinyl}amino)-benzenesulfonamide (8).* Compound **8** was prepared from 3-[(6-chloro-4-pyrimidinyl)amino]-*N*-methylbenzenesulfonamide and 2-methylaniline using Method A as a white solid in 19% yield (52 mg): $^1$H NMR (400 MHz, DMSO-$d_6$) $\delta$ 9.85 (br. s., 1H), 9.21 (br. s., 1H), 8.34 (s, 1H), 8.03 (br. s., 1H), 7.80 (d, $J$ = 8.03 Hz, 1H), 7.50−7.57 (m, 1H), 7.42−7.49 (m, 1H), 7.40 (d, $J$ = 7.53 Hz, 1H), 7.19−7.37 (m, 4H), 5.82 (s, 1H), 2.43 (d, $J$ = 4.77 Hz, 3H), 2.23 (s, 3H). MS ($m/z$) 370.1 (M + H$^+$).

*N-Methyl-3-[(6-{[2-(methyloxy)phenyl]amino}-4-pyrimidinyl)-amino]benzenesulfonamide (9).* Compound **9** was prepared from 3-[(6-chloro-4-pyrimidinyl)amino]-*N*-methylbenzenesulfonamide and 2-methoxyaniline using Method A in 85% yield (345 mg): $^1$H NMR (400 MHz, DMSO-$d_6$) $\delta$ 9.46 (s, 1H), 8.45 (s, 1H), 8.26 (s, 1H), 8.10 (s, 1H), 7.88 (d, $J$ = 8.28 Hz, 1H), 7.67 (d, $J$ = 7.53 Hz, 1H), 7.49 (t, $J$ = 7.91 Hz, 1H), 7.38−7.44 (m, 1H), 7.30 (d, $J$ = 7.78 Hz, 1H), 7.04−7.16 (m, 2H), 6.91−7.00 (m, 1H), 6.07 (s, 1H), 3.83 (s, 3H), 2.44 (d, $J$ = 5.02 Hz, 3H). MS ($m/z$) 386.1 (M + H$^+$).

*3-({6-[(3-Chlorophenyl)amino]-4-pyrimidinyl}amino)-N-methyl-benzenesulfonamide Trifluoroacetate (10).* Compound **10** was prepared from 6-chloro-*N*-(3-chlorophenyl)-4-pyrimidinamine and 3-amino-*N*-methylbenzenesulfonamide using Method A as a white solid in 38% yield (126 mg): $^1$H NMR (400 MHz, DMSO-$d_6$) $\delta$ 9.68 (s, 1H), 9.54 (s, 1H), 8.41 (s, 1H), 8.09 (t, $J$ = 1.88 Hz, 1H), 7.90−7.94 (m, 1H), 7.88 (t, $J$ = 2.01 Hz, 1H), 7.53 (t, $J$ = 7.91 Hz, 1H), 7.41−7.49 (m, 2H), 7.29−7.39 (m, 2H), 7.03 (dd, $J$ = 1.25, 8.03 Hz, 1H), 6.21 (s, 1H), 2.45 (d, $J$ = 4.77 Hz, 3H). MS ($m/z$) 390.1 (M + H$^+$).

*N-Methyl-3-[(6-{[3-(methyloxy)phenyl]amino}-4-pyrimidinyl)-amino]benzenesulfonamide Trifluoroacetate (11).* Compound **11** was prepared from 3-[(6-chloro-4-pyrimidinyl)amino]-*N*-methylben-zenesulfonamide and 3-(methyloxy)aniline using Method A as a pale yellow solid in 32% yield (70 mg): $^1$H NMR (400 MHz, DMSO-$d_6$) $\delta$ 9.77 (s, 1H), 9.49 (br. s., 1H), 8.38 (s, 1H), 8.06 (s, 1H), 7.88 (d, $J$ = 8.28 Hz, 1H), 7.54 (t, $J$ = 7.91 Hz, 1H), 7.46 (q, $J$ = 4.68 Hz, 1H), 7.38 (d, $J$ = 7.78 Hz, 1H), 7.21−7.29 (m, 1H), 7.18 (s, 1H), 7.09 (d, $J$ = 8.03 Hz, 1H), 6.65 (dd, $J$ = 2.01, 8.03 Hz, 1H), 6.22 (s, 1H), 3.76 (s, 3H), 2.44 (d, $J$ = 4.77 Hz, 3H). MS ($m/z$) 386.1 (M + H$^+$).

*N-Methyl-3-[(6-{[3-(methylsulfonyl)phenyl]amino}-4-pyrimidinyl)amino]benzenesulfonamide Trifluoroacetate (12).* Compound **12** was prepared from 3-[(6-chloro-4-pyrimidinyl)-amino]-*N*-methylbenzenesulfonamide and 3-(methylsulfonyl)aniline using Method A as a white solid in 27% yield (62 mg): $^1$H NMR (400 MHz, DMSO-$d_6$) $\delta$ 9.79 (s, 1H), 9.74 (s, 1H), 8.43 (s, 1H), 8.21 (s, 1H), 8.08 (s, 1H), 7.99 (d, $J$ = 7.78 Hz, 1H), 7.93 (d, $J$ = 8.03 Hz, 1H), 7.49−7.63 (m, 3H), 7.43−7.49 (m, 1H), 7.37 (d, $J$ = 7.78 Hz, 1H), 6.24 (s, 1H), 3.22 (s, 3H), 2.45 (d, $J$ = 4.52 Hz, 3H). MS ($m/z$) 434.1 (M + H$^+$).

*N-Methyl-3-({6-[(4-methylphenyl)amino]-4-pyrimidinyl}amino)-benzenesulfonamide Hydrochloride (14).* Compound **14** was prepared from 3-[(6-chloro-4-pyrimidinyl)amino]-*N*-methylbenzene-sulfonamide and 4-methylaniline using Method A as a white solid in 15% yield (7.8 mg): $^1$H NMR (400 MHz, DMSO-$d_6$) $\delta$ 9.49 (s, 1H), 9.13 (s, 1H), 8.30 (s, 1H), 8.07−8.14 (m, 1H), 7.85−7.92 (m, 1H), 7.50 (t, $J$ = 8.03 Hz, 1H), 7.37−7.46 (m, 3H), 7.31 (d, $J$ = 7.78 Hz,

1H), 7.13 (d, J = 8.28 Hz, 2H), 6.15 (s, 1H), 2.44 (d, J = 5.02 Hz, 3H), 2.27 (s, 3H). MS (m/z) 370.1 (M + H+).

*N-Methyl-3-[(6-{[4-(methyloxy)phenyl]amino}-4-pyrimidinyl)-amino]benzenesulfonamide Hydrochloride (15).* Compound **15** was prepared from 3-[(6-chloro-4-pyrimidinyl)amino]-N-methylbenzene-sulfonamide and 4-(methyloxy)aniline using Method A as an off-white solid in 50% yield (100 mg): 1H NMR (400 MHz, DMSO-$d_6$) δ 10.28 (br. s., 1H), 9.96 (br. s., 1H), 8.42 (s, 1H), 7.99 (s, 1H), 7.77 (d, J = 8.03 Hz, 1H), 7.51−7.62 (m, 2H), 7.47 (d, J = 7.78 Hz, 1H), 7.35 (d, J = 8.78 Hz, 2H), 7.01 (d, J = 8.78 Hz, 2H), 6.12 (s, 1H), 2.43 (d, J = 4.77 Hz, 3H). MS (m/z) 386.1 (M + H+).

*N-Methyl-3-[(6-{[4-(methylsulfonyl)phenyl]amino}-4-pyrimidinyl)amino]benzenesulfonamide Trifluoroacetate (16).* Compound **16** was prepared from 3-[(6-chloro-4-pyrimidinyl)-amino]-N-methylbenzenesulfonamide and 4-(methylsulfonyl)aniline using Method A as a white solid in 69% yield (143 mg): 1H NMR (400 MHz, DMSO-$d_6$) δ 9.85 (s, 1H), 9.72 (s, 1H), 8.45 (s, 1H), 8.09−8.12 (m, 1H), 7.93 (dd, J = 1.76, 8.03 Hz, 1H), 7.80−7.91 (m, 4H), 7.54 (t, J = 7.91 Hz, 1H), 7.45 (q, J = 5.02 Hz, 1H), 7.37 (d, J = 7.78 Hz, 1H), 6.30 (s, 1H), 3.16 (s, 3H), 2.45 (d, J = 5.02 Hz, 3H). MS (m/z) 434.0 (M + H+).

*N-Methyl-3-((2-(m-tolylamino)pyridin-4-yl)amino)-benzenesulfonamide Trifluoroacetate (17).* A mixture of 2,4-dichloropyridine (50 mg, 0.34 mmol) and 3-amino-N-methylbenze-nesulfonamide (63 mg, 0.34 mmol) in i-PrOH (2 mL) was treated with 1 M aqueous HCl (0.34 mL, 0.34 mmol) and stirred at 80 °C for 60 h before being cooled to room temperature. The mixture was subjected to reverse phase HPLC to give 3-((2-chloropyridin-4-yl)amino)-N-methylbenzenesulfonamide as a white solid (59 mg, 42% yield): 1H NMR (400 MHz, DMSO-$d_6$) δ 9.47 (s, 1H), 8.08 (d, J = 5.52 Hz, 1H), 7.58−7.63 (m, 1H), 7.44−7.58 (m, 4H), 6.91−6.98 (m, 2H), 2.45 (d, J = 4.77 Hz, 3H). MS (m/z) 298.0 (M + H+).

A mixture of 3-((2-chloropyridin-4-yl)amino)-N-methylbenzenesul-fonamide (30 mg, 0.07 mmol) and m-toluidine (0.03 mL, 0.28 mmol) in i-PrOH (2 mL) was treated with 1 M aqueous HCl (0.1 mL, 0.1 mmol) and subjected to microwave irradiation (150 °C) for 60 min before being cooled to room temperature and subjected to reverse phase HPLC to give **17** as a white solid (16 mg, 45% yield): 1H NMR (400 MHz, DMSO-$d_6$) δ 12.40 (br. s., 1H), 10.10 (br. s., 1H), 9.85 (br. s., 1H), 7.77 (d, J = 7.28 Hz, 1H), 7.65−7.72 (m, 1H), 7.52−7.63 (m, 4H), 7.30−7.38 (m, 1H), 7.05−7.15 (m, 3H), 6.59 (dd, J = 2.26, 7.28 Hz, 1H), 6.40 (d, J = 2.26 Hz, 1H), 2.42 (d, J = 4.77 Hz, 3H), 2.34 (s, 3H). MS (m/z) 369.1 (M + H+).

*N-Methyl-3-((2-(m-tolylamino)pyrimidin-4-yl)amino)-benzenesulfonamide Trifluoroacetate (18).* A mixture of 2,4-dichloropyrimidine (160 mg, 1.1 mmol) and 3-amino-N-methylbenze-nesulfonamide (100 mg, 0.5 mmol) in i-PrOH (4 mL) was treated with Na$_2$CO$_3$ (171 mg, 1.6 mmol) and stirred at 80 °C for 60 h before being cooled to room temperature and filtered. The filtrate was concentrated and subjected to flash column chromatography (50−75% EtOAc-hexanes) to give 3-((2-chloropyrimidin-4-yl)amino)-N-meth-ylbenzenesulfonamide as a pale yellow solid (133 mg, 60% yield): 1H NMR (400 MHz, DMSO-$d_6$) δ 9.47 10.36 (br. s., 1H), 8.24 (d, J = 5.77 Hz, 1H), 8.07 (s, 1H), 7.85−7.94 (m, 1H), 7.61 (t, J = 8.03 Hz, 1H), 7.47 (d, J = 8.28 Hz, 2H), 6.81 (d, J = 5.77 Hz, 1H), 2.48 (s, 3H). MS (m/z) 299.0 (M + H+).

A mixture of 3-((2-chloropyrimidin-4-yl)amino)-N-methylbenzene-sulfonamide (60 mg, 0.2 mmol) and m-toluidine (0.043 mL, 0.4 mmol) was treated with 1 M aqueous HCl (0.2 mL, 0.2 mmol) and stirred at 80 °C for 60 min before being cooled to room temperature, concentrated, and subjected to reverse phase HPLC to give **18** as a white solid (70 mg, 71% yield): 1H NMR (400 MHz, DMSO-$d_6$) δ 10.53 (br. s., 1H), 9.97 (br. s., 1H), 8.26 (d, J = 7.28 Hz, 1H), 8.02 (d, J = 6.78 Hz, 1H), 7.74 (s, 1H), 7.48−7.58 (m, 3H), 7.31−7.42 (m, 2H), 7.22−7.30 (m, 1H), 6.97 (d, J = 7.28 Hz, 1H), 6.38 (d, J = 6.78 Hz, 1H), 2.43 (d, J = 5.02 Hz, 3H), 2.29 (s, 3H). MS (m/z) 370.1 (M + H+).

*N-Methyl-3-({4-[(3-methylphenyl)amino]-1,3,5-triazin-2-yl}-amino)benzenesulfonamide (19).* A mixture of 2,4,6-trichloro-1,3,5-triazine (800 mg, 4.3 mmol) in AcOH (13 mL) at 15 °C was treated

with a solution of 3-amino-N-methylbenzenesulfonamide (808 mg, 4.3 mmol) in AcOH (1.6 mL) and H$_2$O (6.8 mL) dropwise over 15 min. The mixture was stirred an additional 10 min before being diluted with saturated aqueous NaCl. The precipitate was collected by filtration, washed with H$_2$O and Et$_2$O, and dried to give 3-[(4,6-dichloro-1,3,5-triazin-2-yl)amino]-N-methylbenzenesulfonamide as an off-white solid (1.05 g, 69% yield): 1H NMR (400 MHz, DMSO-$d_6$) δ 11.35−11.47 (m, 1H), 8.07−8.15 (m, 1H), 7.84 (d, J = 7.53 Hz, 1H), 7.60−7.69 (m, 1H), 7.50−7.60 (m, 2H), 2.44−2.49 (m, 3H). MS (m/z) 334.0 (M + H+).

A mixture of 3-[(4,6-dichloro-1,3,5-triazin-2-yl)amino]-N-methyl-benzenesulfonamide (160 mg, 0.48 mmol) in AcOH (4 mL) and H$_2$O (1 mL) was treated with 3-methylaniline (56 mg, 0.53 mmol) and NaOAc (47 mg, 0.58 mmol) and stirred at room temperature overnight. The mixture was diluted with saturated aqueous NaCl, and the precipitate was collected by filtration and washed twice with H$_2$O. The filtered solid was dissolved in Et$_2$O and the solution concentrated to give 3-({4-chloro-6-[(3-methylphenyl)amino]-1,3,5-triazin-2-yl}-amino)-N-methylbenzenesulfonamide as a white solid (166 mg, 86% yield): 1H NMR (400 MHz, DMSO-$d_6$) δ 10.53 (br. s., 1H), 10.30 (br. s., 1H), 8.12 (br. s., 1H), 7.96 (br. s., 1H), 7.78 (br. s., 1H), 7.52−7.65 (m, 1H), 7.48 (d, J = 7.53 Hz, 4H), 7.24 (t, J = 7.78 Hz, 1H), 6.92 (d, J = 7.28 Hz, 1H), 2.44 (br. s., 3H), 2.29 (br. s., 3H). MS (m/z) 405.0 (M + H+).

A mixture of 3-({4-chloro-6-[(3-methylphenyl)amino]-1,3,5-triazin-2-yl}amino)-N-methylbenzenesulfonamide (166 mg, 0.41 mmol) in EtOH (1 mL) was treated with ammonium formate (129 mg, 2.1 mmol) and 10% palladium on carbon (44 mg, 0,04 mmol) and stirred at 80 °C for 1 h before being cooled and filtered through Celite and washed with EtOH and then DMSO. The filtrate was subjected to reverse phase HPLC to give **19** as a white solid (60 mg, 38%): 1H NMR (400 MHz, DMSO-$d_6$) δ 10.07 (br. s., 1H), 9.80 (br. s., 1H), 8.40 (s, 1H), 8.18 (br. s. 1H), 7.50−7.61 (m, 3H), 7.38−7.50 (m, 2H), 7.22 (t, J = 7.91 Hz, 1H), 6.88 (d, J = 7.53 Hz, 1H), 2.44 (d, J = 5.02 Hz, 3H), 2.30 (s, 3H). MS (m/z) 405.0 (M + H+).

*3-({4-[(4-Chlorophenyl)amino]-1,3,5-triazin-2-yl}amino)-N-meth-ylbenzenesulfonamide (20).* A mixture of 3-[(4,6-dichloro-1,3,5-triazin-2-yl)amino]-N-methylbenzenesulfonamide (160 mg, 0.48 mmol) in AcOH (4 mL) and H$_2$O (1 mL) was treated with 4-chloroaniline (73 mg, 0.58 mmol) and NaOAc (47 mg, 0.58 mmol) and stirred at room temperature overnight. The mixture was diluted with saturated aqueous NaCl, and the precipitate was collected by filtration and washed with water. The filtered solid was dissolved in Et$_2$O, and the solution was concentrated to give 3-({4-chloro-6-[(4-chlorophenyl)amino]-1,3,5-triazin-2-yl}amino)-N-methylbenzenesul-fonamide as a white solid (230 mg, 100% yield): MS (m/z) 425.0 (M + H+).

A mixture of 3-({4-chloro-6-[(4-chlorophenyl)amino]-1,3,5-triazin-2-yl}amino)-N-methylbenzenesulfonamide (230 mg, 0.49 mmol) in EtOH (1.2 mL) was treated with ammonium formate (153 mg, 2.4 mmol) and 10% palladium on carbon (52 mg, 0.05 mmol) and stirred at 60 °C for 30 min before being cooled to room temperature. The mixture was diluted with DMSO (15 mL) and filtered through Celite, and the filtrate was subjected to reverse HPLC to give **20** as a pale pink solid (39 mg, 19% yield): 1H NMR (400 MHz, DMSO-$d_6$) δ 10.13 (br. s., 1H), 10.00 (br. s., 1H), 8.43 (br. s., 1H), 8.08 (br. s., 2H), 7.79 (br. s., 2H), 7.57 (t, J = 7.91 Hz, 1H), 7.41−7.52 (m, 2H), 7.38 (d, J = 8.53 Hz, 1H), 2.44 (d, J = 4.52, 3H). MS (m/z) 391.0 (M + H+).

*3-({6-[(5-Chloro-2-pyridinyl)amino]-4-pyrimidinyl}amino)-N-methylbenzenesulfonamide Trifluoroacetate (21).* Compound **21** was prepared from 3-[(6-chloro-4-pyrimidinyl)amino]-N-methylben-zenesulfonamide and 5-chloro-2-pyridinamine using Method B as a pale yellow solid in 6% yield (22 mg): 1H NMR (400 MHz, DMSO-$d_6$) δ 10.32 (br. s., 1H), 9.97 (br. s., 1H), 8.44 (s, 1H), 8.31 (d, J = 2.51 Hz, 1H), 8.18 (s, 1H), 7.88−7.94 (m, 1H), 7.85 (dd, J = 2.64, 8.91 Hz, 1H), 7.51−7.59 (m, 2H), 7.46 (q, J = 4.85 Hz, 1H), 7.38 (d, J = 7.78 Hz, 1H), 7.24 (s, 1H), 2.45 (d, J = 5.02 Hz, 3H). MS (m/z) 390.9 (M + H+).

*N-Methyl-3-[(6-{[5-(trifluoromethyl)-2-pyridinyl]amino}-4-pyrimidinyl)amino]benzenesulfonamide Trifluoroacetate (22).* Compound **22** was prepared from 3-[(6-chloro-4-pyrimidinyl)-amino]-*N*-methylbenzenesulfonamide and 5-(trifluoromethyl)-2-pyridinamine using Method B as a pale yellow solid in 17% yield (69 mg): $^1$H NMR (400 MHz, DMSO-$d_6$) $\delta$ 10.57 (br. s., 1H), 9.98 (s, 1H), 8.62 (s, 1H), 8.48 (s, 1H), 8.20 (s, 1H), 8.05–8.12 (m, 1H), 7.93 (d, *J* = 8.03 Hz, 1H), 7.72 (d, *J* = 8.78 Hz, 1H), 7.55 (t, *J* = 8.03 Hz, 1H), 7.46 (q, *J* = 4.60 Hz, 1H), 7.35–7.42 (m, 2H), 2.46 (d, *J* = 4.77 Hz, 3H). MS (*m/z*) 424.9 (M + H$^+$).

*N-Methyl-3-[(6-{[3-(1-methylethyl)phenyl]amino}-4-pyrimidinyl)-amino]benzenesulfonamide (23).* Compound **23** was prepared from 3-[(6-chloro-4-pyrimidinyl)amino]-*N*-methylbenzenesulfonamide and 3-(1-methylethyl)aniline using Method A as an off-white solid in 12% yield (25 mg): $^1$H NMR (400 MHz, DMSO-$d_6$) $\delta$ 9.49 (br. s., 1H), 9.15 (br. s., 1H), 8.31 (s, 1H), 8.08 (s, 1H), 7.90 (d, *J* = 7.32 Hz, 1H), 7.46–7.53 (m, 1H), 7.44 (d, *J* = 7.81 Hz, 1H), 7.39 (q, *J* = 4.80 Hz, 1H), 7.29–7.34 (m, 2H), 7.22 (t, *J* = 7.81 Hz, 1H), 6.89 (d, *J* = 7.57 Hz, 1H), 6.18 (s, 1H), 2.86 (dt, *J* = 6.93, 13.73 Hz, 1H), 2.44 (d, *J* = 5.13 Hz, 3H), 1.22 (s, 3H), 1.20 (s, 3H). MS (*m/z*) 398.0 (M + H$^+$).

*3-[(6-{[3-(1,1-Dimethylethyl)phenyl]amino}-4-pyrimidinyl)-amino]-N-methylbenzenesulfonamide Trifluoroacetate (24).* Compound **24** was prepared from 3-[(6-chloro-4-pyrimidinyl)amino]-*N*-methylbenzenesulfonamide and 3-(1,1-dimethylethyl)aniline using Method A as a white solid in 53% yield (148 mg): $^1$H NMR (400 MHz, DMSO-$d_6$) $\delta$ 9.72 (br. s., 1H), 9.42 (br. s., 1H), 8.36 (s, 1H), 8.03 (s, 1H), 7.86 (d, *J* = 8.06 Hz, 1H), 7.53 (t, *J* = 7.93 Hz, 1H), 7.35–7.46 (m, 4H), 7.28 (t, *J* = 7.81 Hz, 1H), 7.11 (d, *J* = 7.81 Hz, 1H), 6.16 (s, 1H), 2.44 (d, *J* = 4.88 Hz, 3H), 1.29 (s, 9H). MS (*m/z*) 412.2 (M + H$^+$).

*3,3′-(4,6-Pyrimidinediyldiimino)bis(N-methylbenzenesulfona-mide) Trifluoroacetate (25).* Compound **25** was prepared from 4,6-dichloropyrimidine (1 equiv) and 3-amino-*N*-methylbenzenesulfona-mide (2 equiv) using Method A as a white solid in 41% yield (81 mg): $^1$H NMR (400 MHz, DMSO-$d_6$) $\delta$ 9.75 (s, 2H), 8.41 (s, 1H), 8.08 (s, 2H), 7.92 (d, *J* = 7.78 Hz, 2H), 7.54 (t, *J* = 7.91 Hz, 2H), 7.46 (q, *J* = 4.85 Hz, 2H), 7.37 (d, *J* = 7.78 Hz, 2H), 6.24 (s, 1H), 2.45 (d, *J* = 4.52 Hz, 6H). MS (*m/z*) 449.1 (M + H$^+$).

*N-Methyl-3-({6-[(3-nitrophenyl)amino]-4-pyrimidinyl}amino)-benzenesulfonamide Trifluoroacetate (26).* Compound **26** was prepared from 3-[(6-chloro-4-pyrimidinyl)amino]-*N*-methylbenzene-sulfonamide and 3-nitroaniline using Method A as a yellow solid in 40% yield (102 mg): $^1$H NMR (400 MHz, DMSO-$d_6$) $\delta$ 9.87 (br. s., 1H), 9.74 (br. s., 1H), 8.71 (br. s., 1H), 8.45 (br. s., 1H), 8.08 (br. s., 1H), 7.99 (d, *J* = 7.53 Hz, 1H), 7.93 (d, *J* = 7.53 Hz, 1H), 7.81 (d, *J* = 7.78 Hz, 1H), 7.49–7.63 (m, 2H), 7.41–7.49 (m, 1H), 7.36 (d, *J* = 7.28 Hz, 1H), 6.25 (br. s., 1H), 2.44 (d, *J* = 2.51 Hz, 3H). MS (*m/z*) 401.0 (M + H$^+$).

*N-Methyl-3-({6-[methyl(3-methylphenyl)amino]-4-pyrimidinyl}-amino)benzenesulfonamide (27).* Compound **27** was prepared from 3-[(6-chloro-4-pyrimidinyl)amino]-*N*-methylbenzenesulfonamide and methyl(3-methylphenyl)amine using Method A as a pale brown solid in 48% yield (60 mg): $^1$H NMR (400 MHz, DMSO-$d_6$) $\delta$ 9.58 (br. s., 1H), 8.38 (s, 1H), 8.07 (s, 1H), 7.77 (d, *J* = 7.28 Hz, 1H), 7.36–7.54 (m, 3H), 7.33 (d, *J* = 7.28 Hz, 1H), 7.10–7.24 (m, 3H), 5.74 (s, 1H), 3.41 (s, 3H), 2.42 (s, 3H), 2.37 (s, 3H). MS (*m/z*) 384.1 (M + H$^+$).

*N-Methyl-3-(methyl{6-[(3-methylphenyl)amino]-4-pyrimidinyl}-amino)benzenesulfonamide (28).* Compound **28** was prepared from 3-[(6-chloro-4-pyrimidinyl)(methyl)amino]-*N*-methylbenzenesulfona-mide and 3-methylaniline using Method A as a white solid in 23% yield (37 mg): $^1$H NMR (400 MHz, DMSO-$d_6$) $\delta$ 9.46 (br. s., 1H), 8.34 (s, 1H), 7.61–7.81 (m, 4H), 7.55 (q, *J* = 4.77 Hz, 1H), 7.12–7.34 (m, 3H), 6.85 (d, *J* = 7.03 Hz, 1H), 5.79 (s, 1H), 3.44 (s, 3H), 2.44 (d, *J* = 5.02 Hz, 3H), 2.26 (s, 3H). MS (*m/z*) 384.1 (M + H$^+$).

*3-({6-[(3-Bromophenyl)amino]-4-pyrimidinyl}amino)-N-methyl-benzenesulfonamide (29).* A mixture of 3-[(6-chloro-4-pyrimidinyl)-amino]-*N*-methylbenzenesulfonamide (15 g, 50 mmol) and 3-bromoaniline (7.8 g, 43 mmol) in isoamylalcohol (10 mL) was treated with HCl (3 mL of a 2 M solution, 6 mmol) and stirred at 131

°C for 6 h. The mixture was cooled and quenched with aqueous NH$_4$OH and stirred for 30 min. The precipitate that formed was collected by filtration, washed with hexanes, and dried to give **29** as a yellow solid (17.5 g, 93% yield): $^1$H NMR (400 MHz, DMSO-$d_6$) $\delta$ 9.67 (br. s., 1H), 9.54 (br. s., 1H), 8.39 (s, 1H), 8.11 (br. s., 1H), 8.03 (br. s., 1H), 7.93 (d, *J* = 7.53 Hz, 1H), 7.41–7.58 (m, 3H), 7.34 (d, *J* = 7.53 Hz, 1H), 7.25 (t, *J* = 7.91 Hz, 1H), 7.13 (d, *J* = 7.28 Hz, 1H), 6.25 (s, 1H), 2.45 (d, *J* = 4.52 Hz, 3H), MS (*m/z*) 436.0 (M + H$^+$).

*3-({6-[(5-Chloro-2-pyridinyl)amino]-4-pyrimidinyl}amino)-N-methyl-4-(methyloxy)-benzenesulfonamide Trifluoroacetate (37).* Compound **37** was prepared from 3-[(6-chloro-4-pyrimidinyl)-amino]-*N*-methyl-4-(methyloxy)benzenesulfonamide and 5-chloro-2-pyridinamine using Method B as a pale yellow solid in 4% yield (22 mg): $^1$H NMR (400 MHz, DMSO-$d_6$) $\delta$ 10.31 (br. s., 1H), 9.15 (br. s., 1H), 8.38 (s, 1H), 8.29–8.31 (m, 1H), 8.26–8.28 (m, 1H), 7.85 (dd, *J* = 9.03, 2.76 Hz, 1H), 7.49–7.56 (m, 2H), 7.30–7.34 (m, 1H), 7.27–7.30 (m, 1H), 7.18 (br. s., 1H), 3.93 (s, 3H), 2.43 (d, *J* = 5.02 Hz, 3H). MS (*m/z*) 421.0 (M + H$^+$).

*3-({6-[(5-Chloro-2-pyridinyl)amino]-4-pyrimidinyl}amino)-N-methyl-4-[(trifluoromethyl)oxy]benzenesulfonamide Trifluoroace-tate (39).* Compound **39** was prepared from 3-[(6-chloro-4-pyrimidinyl)amino]-*N*-methyl-4-[(trifluoromethyl)oxy]-benzenesulfonamide and 5-chloro-2-pyridinamine using Method B as a pale brown solid in 25% yield (123 mg): $^1$H NMR (400 MHz, DMSO-$d_6$) $\delta$ 10.31 (br. s., 1H), 9.62 (s, 1H), 8.44 (d, *J* = 2.01 Hz, 1H), 8.37 (s, 1H), 8.31 (d, *J* = 2.26 Hz, 1H), 7.85 (dd, *J* = 8.91, 2.64 Hz, 1H), 7.54–7.68 (m, 4H), 7.33 (s, 1 H), 2.49 (d, *J* = 4.77 Hz, 3H). MS (*m/z*) 475.0 (M + H$^+$).

*3-({6-[(5-Chloro-2-pyridinyl)amino]-4-pyrimidinyl}amino)-N-methyl-4-[(2,2,2-trifluoroethyl)oxy]benzenesulfonamide Trifluoroa-cetate (41).* Compound **41** was prepared from 3-[(6-chloro-4-pyrimidinyl)amino]-*N*-methyl-4-[(2,2,2-trifluoroethyl)oxy]-benzenesulfonamide and 5-chloro-2-pyridinamine using Method B as a pale yellow solid in 12% yield (49 mg): $^1$H NMR (400 MHz, DMSO-$d_6$) $\delta$ 10.49 (br. s., 1H), 9.47 (br. s., 1H), 8.38 (s, 1H), 8.31 (d, *J* = 2.51 Hz, 1H), 8.01 (d, *J* = 2.01 Hz, 1H), 7.87 (dd, *J* = 8.91, 2.64 Hz, 1H), 7.62 (dd, *J* = 8.66, 2.13 Hz, 1H), 7.49 (d, *J* = 8.78 Hz, 1H), 7.42–7.47 (m, 2H), 7.05 (br. s., 1H), 4.92 (q, *J* = 8.78 Hz, 2H), 2.44 (d, *J* = 5.02 Hz, 3H). MS (*m/z*) 489.0 (M + H$^+$).

*3-({6-[(5-Chloro-2-pyridinyl)amino]-4-pyrimidinyl}amino)-N-methyl-4-(methylsulfonyl)benzenesulfonamide (42).* Compound **42** was prepared from 3-[(6-chloro-4-pyrimidinyl)amino]-*N*-methyl-4-(methylsulfonyl)benzenesulfonamide and 5-chloro-2-pyridinamine using Method B as an off-white solid in 11% yield (36 mg): $^1$H NMR (400 MHz, DMSO-$d_6$) $\delta$ 10.26 (s, 1H), 9.08–9.10 (m, 1H), 8.45–8.48 (m, 1H), 8.38–8.40 (m, 1H), 8.31–8.34 (m, 1H), 8.12 (d, *J* = 8.28 Hz, 1H), 7.84 (dd, *J* = 2.76, 9.03 Hz, 1H), 7.80 (q, *J* = 4.52 Hz, 1H), 7.68 (dd, *J* = 1.76, 8.28 Hz, 1H), 7.61 (d, *J* = 9.03 Hz, 1H), 7.42 (s, 1H), 3.33 (s, 3H), 2.50 (d, 3H, obscured by solvent). MS (*m/z*) 469.0 (M + H$^+$).

*3-({6-[(5-chloro-2-pyridinyl)amino]-4-pyrimidinyl}amino)-4-(eth-ylsulfonyl)-N-methylbenzenesulfonamide p-Toluenesulfonate Monohydrate (43).* A mixture of 3-[(6-chloro-4-pyrimidinyl)amino]-4-(ethylsulfonyl)-*N*-methylbenzenesulfonamide (1.5 g, 3.84 mmol), 5-chloro-2-pyridinamine (0.99 g, 7.68 mmol), Cs$_2$CO$_3$ (3.75 g, 11.5 mmol), BINAP (0.096 g, 0.154 mmol), and Pd(OAc)$_2$ (0.034 g, 0.154 mmol) in 1,4-dioxane (6.4 mL) was treated with a few drops of DMF (to solubilize the reagents) and subjected to microwave irradiation (150 °C) for 30 min before being cooled to room temperature and filtered. This procedure was repeated nine times, and the filtrates from all reactions were combined and concentrated. The residue was suspended in CH$_2$Cl$_2$, and the resulting solid was collected by filtration, triturated in MeOH (3 × 50 mL), triturated in acetone (3 × 50 mL), and then collected and dried to give **43** as a crystalline free base (7.8 g, 42% yield). The resulting crystalline free base product was converted to the *p*-TsOH salt as this produced an amorphous form that maximized oral bioavailability for *in vivo* studies. Thus, 2 g of crystalline free base was suspended in ~50 mL of MeCN/MeOH (2:1) and treated with *p*-TsOH·H$_2$O (796 mg, 1 equiv), and the resulting solution was heated at 60 °C for 15 min to give a clear solution. The solution was concentrated, the residue was dissolved in

$CH_2Cl_2$, and the resulting solution was concentrated to give the amorphous salt. This process was repeated in multiple 1−2 g batches for the remaining material, and the batches were combined and mixed by mortar and pestle to give the *p*-TsOH salt of **43** as a pale yellow solid (8.16 g, 77%): $^1H$ NMR (500 MHz, DMSO-$d_6$) δ 10.67 (br. s., 1H, C6-aniline-NH), 9.58 (br. s., 1H, C4-aniline-NH), 8.47 (s, 1H, pyrimidine C2−H), 8.29−8.38 (m, 2H, pyridine C6−H, benzene-sulfonamide C2−H), 8.14 (d, *J* = 8.31 Hz, 1H, benzenesulfonamide C5−H), 7.91 (dd, *J* = 2.32, 8.93 Hz, 1H, pyridine C4−H), 7.77−7.85 (m, 2H, sulfonamide-NH, benzenesulfonamide C6−H), 7.45−7.53 (m, 3H, pyridine C3−H, *p*-TsOH−C2-H/C6−H), 7.23 (br. s., 1H, pyrimidine C5−H), 7.12 (d, *J* = 7.83 Hz, 2H. *p*-TsOH−C3-H/C5−H), 3.41 (q, *J* = 7.34 Hz, 2H, $SO_2CH_2CH_3$), 2.49−2.51 (m, 3H, $SO_2NHCH_3$), 2.30 (s, 3H, p-TsOH-$CH_3$), 1.11 (t, *J* = 7.34 Hz, 3H, $SO_2CH_2CH_3$). $^{13}C$ NMR (500 MHz, DMSO-$d_6$) δ 155.5 (pyrimidine-C2), 152.73 (pyridine-C2), 146.60 (*p*-TsOH-C1), 146.24 (pyridine-C6), 145.89 (benzenesulfonamide-C3), 139.00 (benzenesulfonamide-C1), 138.60 (pyridine-C4), 138.45 (*p*-TsOH-C4), 132.70 (benzene-sulfonamide-C5), 128.92 (*p*-TsOH-C3/C5), 126.36 (*p*-TsOH-C2/C6), 125.5 (benzenesulfonamide-C2), 124.67 (pyridine-C5), 124.0 (benzenesulfonamide-C6), 115.49 (pyridine-C3), 92.0 (pyrimidine-C5), 49.77 ($SO_2CH_2CH_3$), 29.57 ($SO_2NHCH_3$), 21.66 (p-TsOH-$CH_3$), 7.74 ($SO_2CH_2CH_3$). $^1H$ and $^{13}C$ NMR resonances were assigned based on gCOSY45, gHMQC, gHMBC, and $^{13}C$ gaspe spectra. Anal. Calcd ($C_{18}H_{19}ClN_6O_4S_2$−$C_7H_8O_3S$−$H_2O$): C, 44.61; H, 4.34; N, 12.48. Found: C, 44.75; H, 4.06; N. 12.35. HRMS ($C_{18}H_{19}ClN_6O_4S_2$) $[M + H]^+$ found *m/z* 483.0676, calcd 483.0676.

*3-[6-(5-Chloro-pyridin-2-ylamino)-pyrimidin-4-ylamino]-N-meth-yl-4-(propane-2-sulfonyl)-benzenesulfonamide (44).* Compound **44** was prepared from 3-[(6-chloro-4-pyrimidinyl)amino]-*N*-methyl-4-[(1-methylethyl)sulfonyl]benzenesulfonamide and 5-chloro-2-pyridin-amine using Method B as a white solid in 40% yield (49 mg): $^1H$ NMR (400 MHz, DMSO-$d_6$) δ 10.49 (br. s., 1H), 9.36 (br. s., 1H), 8.41 (s, 1H), 8.39 (d, *J* = 1.54 Hz, 1H), 8.30 (d, *J* = 2.65 Hz, 1H), 8.06 (d, *J* = 8.38 Hz, 1H), 7.84 (dd, *J* = 2.65, 8.82 Hz, 1H), 7.78 (q, 1H), 7.69 (dd, *J* = 1.65, 8.27 Hz, 1H), 7.52 (d, *J* = 8.82 Hz, 1H), 7.28 (s, 1H), 3.45−3.54 (m, 1H), 2.47 (d, 3H, obscured by solvent), 1.14 (d, *J* = 6.62 Hz, 6H). MS (*m/z*) 496.9 (M + H⁺).

*4-(tert-Butylsulfonyl)-3-(6-(5-chloropyridin-2-ylamino)pyrimidin-4-ylamino)-N-methylbenzenesulfonamide Trifluoroacetate (45).* Compound **45** was prepared from 3-[(6-chloro-4-pyrimidinyl)-amino]-4-[(1,1-dimethylethyl)sulfonyl]-*N*-methylbenzenesulfonamide and 5-chloro-2-pyridinamine using Method B as a pale yellow solid in 50% yield (61 mg): $^1H$ NMR (400 MHz, DMSO-$d_6$) δ 10.27 (s, 1H), 9.28 (s, 1H), 8.61 (d, *J* = 1.54 Hz, 1H), 8.40 (s, 1H), 8.32 (d, *J* = 2.43 Hz, 1H), 7.98 (d, *J* = 8.38 Hz, 1H), 7.76−7.83 (m, 2H), 7.55−7.60 (m, 2H), 7.40 (s, 1H), 2.47 (d, 3H, obscured by solvent), 1.22 (s, 9H). MS (*m/z*) 511.2 (M + H⁺).

**Computational Modeling.** The crystal structure of **4** bound to TNNI3K (PDB 6B5J) reported in this article was used to model the binding of compounds **3**, **37**, and **43** to TNNI3K. The crystal structure PDB 4I23 was used to model the binding of **3** to EGFR, and the crystal structure PDB 4YHT was used to model the binding of **37** and **43** to B-raf. All computational modeling was performed using Maestro from Schrödinger Release 2017−1 (Schrödinger, LLC, New York, 2017). Protein structures were prepared using the Protein Preparation Wizard using default parameters. Protons were added, water orientations were sampled, and hydrogen bond assignments were optimized. Final hydrogen orientations were optimized by performing a restrained minimization with heavy atoms kept fixed.

Receptor grids to be used as inputs for Glide were generated around the crystallized ligands in the respective protein structures. Hydrogen bond constraints were defined for the backbone carbonyl and NH of the hinge residue in TNNI3K (Ile542), EGFR (Met793), and B-raf (Cys531). The crystallographic water molecule that is observed to make hydrogen bond interactions with the sulfonyl oxygen of the crystallized ligand and the protein in the back pocket of TNNI3K and B-raf was included in the receptor grids for those targets. Glide XP was used to dock the ligands into the respective structures using default parameters with the exception that enhanced planarity of

conjugated pi groups was enforced. The hydrogen bonding constraints to the hinge residues described above were used to guide the automatic selection of poses. Postdocking minimization was performed with strain correction terms applied. Glide XP scores and visual inspection were used to select reported poses for **3**, **37**, and **43** bound to TNNI3K and **37** and **43** bound to B-raf.

Given that compound **3** is relatively different from the compound crystallized to EGFR and those crystallized to TNNI3K and B-raf, the resultant Glide XP poses of **3** bound to EGFR were further optimized with Prime MM-GBSA using the VSGB solvation model and OPLS3 force field. Ligand poses from Glide XP and receptor residues within 5 Å of these poses were minimized to relieve steric clashes. Prime MM-GBSA scores and visual inspection were used to select the final pose of **3** bound to EGFR.

All structure figures were generated with PyMOL version 1.8.6.0 (Schrödinger, LLC, New York, 2017).

## ■ ASSOCIATED CONTENT

### Ⓢ Supporting Information

The Supporting Information is available free of charge on the ACS Publications website at DOI: 10.1021/acs.jmed-chem.8b00125.

> Kinase selectivity results for **3**, **33**, and **43**, table of statistics for X-ray crystal structures and tabulated data used to generate Figure 4 (PDF)
> Coordinates for docking models of compound **3** (PDB, PDB), compound **37** (PDB, PDB), and compound **43** (PDB, PDB)
> SMILES representation of compounds with key data (CSV)

### Accession Codes

PDB code: 6B5J (TNNI3K-**4**).

## ■ AUTHOR INFORMATION

### Corresponding Author

*E-mail: brian.2.lawhorn@gsk.com. Phone: 484-923-3513.

### ORCID ⓞ

Brian G. Lawhorn: 0000-0003-4618-5314

### Notes

The authors declare the following competing financial interest(s): Authors affiliated with GlaxoSmithKline have received compensation in the form of salary and stock.

## ■ ABBREVIATIONS USED

TNNI3K, troponin I-interacting kinase; EGFR, epidermal growth factor receptor; DNAUC, dose-normalized area under the curve; Cl, iv clearance; F, oral bioavailability; Vdss, volume of distribution; μwave, microwave; TPSA, topological polar surface area; Fu, fraction unbound as percent; Xantphos, 4,5-Bis(diphenylphosphino)-9,9-dimethylxanthene; dba, dibenzyli-deneacetone; BINAP, 2,2′-Bis(diphenylphosphino)-1,1′-bi-naphthyl

## ■ REFERENCES

(1) Zhao, Y.; Meng, X. M.; Wei, Y. J.; Zhao, X. W.; Liu, D. Q.; Cao, H. Q.; Liew, C. C.; Ding, J. F. Cloning and characterization of a novel

cardiac-specific kinase that interacts specifically with cardiac troponin I. *J. Mol. Med. (Heidelberg, Ger.)* **2003**, *81*, 297−304.

(2) (a) Lal, H.; Ahmad, F.; Parikh, S.; Force, T. Troponin I-interacting protein kinase: a novel cardiac-specific kinase, emerging as a molecular target for the treatment of cardiac disease. *Circ. J.* **2014**, *78*, 1514−1519. (b) Milano, A.; Lodder, E. M.; Bezzina, C. R. TNNI3K in cardiovascular disease and prospects for therapy. *J. Mol. Cell. Cardiol.* **2015**, *82*, 167−173.

(3) (a) Wheeler, F. C.; Tang, H.; Marks, O. A.; Hadnott, T. N.; Chu, P. L.; Mao, L.; Rockman, H. A.; Marchuk, D. A. *Tnni3k* modifies disease progression in murine models of cardiomyopathy. *PLoS Genet.* **2009**, *5*, e1000647. (b) Tang, H.; Xiao, K.; Mao, L.; Rockman, H. A.; Marchuk, D. A. Overexpression of TNNI3K, a cardiac-specific MAPKKK, promotes cardiac dysfunction. *J. Mol. Cell. Cardiol.* **2013**, *54*, 101−111. (c) Abraham, D. M.; Marchuk, D. A. Inhibition of the cardiomyocyte-specific troponin I-interacting kinase limits oxidative stress, injury, and adverse remodeling due to ischemic heart disease. *Circ. Res.* **2014**, *114*, 938−940.

(4) Vagnozzi, R. J.; Gatto, G. J., Jr.; Kallander, L. S.; Hoffman, N. E.; Mallilankaraman, K.; Ballard, V. L. T.; Lawhorn, B. G.; Stoy, P.; Philp, J.; Graves, A. P.; Naito, Y.; Lepore, J. J.; Gao, E.; Madesh, M.; Force, T. Inhibition of the cardiomyocyte-specific TNNI3K limits oxidative stress, injury, and adverse remodeling in the ischemic heart. *Sci. Transl. Med.* **2013**, *5*, 207ra141.

(5) Mudd, J. O.; Kass, D. A. Tackling heart failure in the twenty-first century. *Nature* **2008**, *451*, 919−928.

(6) Kaye, D. M.; Krum, H. Drug discovery for heart failure: a new era or the end of the pipeline? *Nat. Rev. Drug Discovery* **2007**, *6*, 127−139.

(7) Harris, P. A.; Boloor, A.; Cheung, M.; Kumar, R.; Crosby, R. M.; Davis-Ward, R. G.; Epperly, A. H.; Hinkle, K. W.; Hunter, R. N., III; Johnson, J. H.; Knick, V. B.; Laudeman, C. P.; Luttrell, D. K.; Mook, R. A.; Nolte, R. T.; Rudolph, S. K.; Szewczyk, J. R.; Truesdale, A. T.; Veal, J. M.; Wang, L.; Stafford, J. A. Discovery of 5-[[4-[(2,3-dimethyl-2*H*-indazol-6-yl)methylamino]-2-pyrimidinyl]amino]-2-methyl-benzene-sulfonamide (pazopanib), a novel and potent vascular endothelial growth factor receptor inhibitor. *J. Med. Chem.* **2008**, *51*, 4632−4640.

(8) (a) Roberts, W. G.; Ung, E.; Whalen, P.; Cooper, B.; Hulford, C.; Autry, C.; Richter, D.; Emerson, E.; Lin, J.; Kath, J.; Coleman, K.; Yao, L.; Martinez-Alsina, L.; Lorenzen, M.; Berliner, M.; Luzzio, M.; Patel, N.; Schmitt, E.; LaGreca, S.; Jani, J.; Wessel, M.; Marr, E.; Griffor, M.; Vajdos, F. Antitumor activity and pharmacology of a selective focal adhesion kinase inhibitor, PF-562,271. *Cancer Res.* **2008**, *68*, 1935−1944. (b) Parsons, J. T.; Slack-Davis, J.; Tilghman, R.; Roberts, W. G. Focal adhesion kinase: targeting adhesion signaling pathways for therapeutic intervention. *Clin. Cancer Res.* **2008**, *14*, 627−232.

(9) (a) Beattie, J. F.; Breault, G. A.; Ellston, R. P. A.; Green, S.; Jewsbury, P. J.; Midgley, C. J.; Naven, R. T.; Minshull, C. A.; Pauptit, R. A.; Tucker, J. A.; Pease, J. E. Cyclin-dependent kinase 4 inhibitors as a treatment for cancer. Part 1: identification and optimization of substituted 4,6-bis anilino pyrimidines. *Bioorg. Med. Chem. Lett.* **2003**, *13*, 2955−2960. (b) Breault, G. A.; Ellston, R. P. A.; Green, S.; James, S. R.; Jewsbury, P. J.; Midgley, C. J.; Pauptit, R. A.; Minshull, C. A.; Tucker, J. A.; Pease, J. E. Cyclin-dependent kinase 4 inhibitors as a treatment for cancer. Part 2: identification and optimization of substituted 2,4-bis anilino pyrimidines. *Bioorg. Med. Chem. Lett.* **2003**, *13*, 2961−2966.

(10) (a) Zhang, Q.; Liu, Y.; Gao, F.; Ding, Q.; Cho, C.; Hur, W.; Jin, Y.; Uno, T.; Joazeiro, C. A. P.; Gray, N. Discovery of EGFR selective 4,6-disubstituted pyrimidines from a combinatorial kinase-directed heterocycle library. *J. Am. Chem. Soc.* **2006**, *128*, 2182−2183. (b) Deng, X.; Okram, B.; Ding, Q.; Zhang, J.; Choi, Y.; Adrian, F. J.; Wojciechowski, A.; Zhang, G.; Che, J.; Bursulaya, B.; Cowan-Jacob, S. W.; Rummel, G.; Sim, T.; Gray, N. S. Expanding the diversity of allosteric Bcr-Abl inhibitors. *J. Med. Chem.* **2010**, *53*, 6934−6946.

(11) (a) Sundberg, T. B.; Choi, H. W.; Song, J.-H.; Russell, C. N.; Hussain, M. M.; Graham, D. B.; Khor, B.; Gagnon, J.; O'Connell, D. J.; Narayan, K.; Dancik, V.; Perez, J. R.; Reinecker, H.-C.; Gray, N. S.; Schreiber, S. L.; Xavier, R. J.; Shamji, A. F. Small-molecule screening identifies inhibition of salt-inducible kinses as therapeutic strategy to enhance immunoregulatory functions of dendritic cells. *Proc. Natl. Acad. Sci. U. S. A.* **2014**, *111*, 12468−12473. (b) Sundberg, T. B.; Liang, Y.; Wu, H.; Choi, H. G.; Kim, N. D.; Sim, T.; Johannessen, L.; Petrone, A.; Khor, B.; Graham, D. B.; Latorre, I. J.; Phillips, A. J.; Schreiber, S. L.; Perez, J.; Shamji, A. F.; Gray, N. S.; Xavier, R. J. Development of chemical probes for investigation of salt-inducible kinase function in vivo. *ACS Chem. Biol.* **2016**, *11*, 2105−2111.

(12) Lawhorn, B. G.; Philp, J.; Zhao, S.; Louer, C.; Hammond, M.; Cheung, M.; Fries, H.; Graves, A. P.; Shewchuk, L.; Wang, L.; Cottom, J. E.; Qi, H.; Zhao, H.; Totoritis, R.; Zhang, G.; Schwartz, B.; Li, H.; Sweitzer, S.; Holt, D. A.; Gatto, G. J., Jr.; Kallander, L. S. Identification of purines and 7-deazapurines as potent and selective type I inhibitors of troponin I-interacting kinase (TNNI3K). *J. Med. Chem.* **2015**, *58*, 7431−7448.

(13) Compound IC$_{50}$ values were determined in a panel of internal kinase assays at GSK at a highest tested concentration of 10 $\mu$M. The composition of the kinase panel was fluid over the course of the project so that compounds were evaluated against an overlapping, but nonidentical number and set of kinases. This data provides a rough approximation of general kinome selectivity for a given compound. For early compounds, a 10-fold selectivity margin was chosen to allow an equitable comparison of general kinase selectivity for weakly active compounds (IC$_{50}$ ≈ 1 $\mu$M) where no greater than 10-fold selectivity could be assessed given the 10 $\mu$M highest test concentration. Selected compounds (**3**, **33**, and **43**) were evaluated in a broader kinase panel and show favorable selectivity using a more stringent 100-fold selectivity measure (see Supporting Information).

(14) (a) Tari, L. W.; Hoffman, I. D.; Bensen, D. C.; Hunter, M. J.; Nix, J.; Nelson, K. J.; McRee, D. E.; Swanson, R. V. Structural basis for the inhibition of Aurora A kinase by a novel class of high affinity disubstituted pyrimidine inhibitors. *Bioorg. Med. Chem. Lett.* **2007**, *17*, 688−691. (b) Zhang, G.; Ren, P.; Gray, N. S.; Sim, T.; Liu, Y.; Wang, X.; Che, J.; Tian, S.-S.; Sandberg, M. L.; Spalding, T. A.; Romeo, R.; Iskandar, M.; Chow, D.; Seidel, H. M.; Karanewsky, D. S.; He, Y. Discovery of pyrimidine benzimidazoles as Lck inhibitors: Part I. *Bioorg. Med. Chem. Lett.* **2008**, *18*, 5618−5621. (c) Ito, A.; Ota, K.; Yoshizawa, K.; Tanaka, K.; Yamabe, T. Ab initio MO study of diphenyl derivatives: diphenylamine, diphenylaminium, diphenylaminyl and diphenylnitroxide. *Chem. Phys. Lett.* **1994**, *223*, 27−34.

(15) (a) Manley, P. J.; Balitza, A. E.; Bilodeau, M. T.; Coll, K. E.; Hartman, G. D.; McFall, R. C.; Rickert, K. W.; Rodman, L. D.; Thomas, K. A. 2,4-disubstituted pyrimidines: A novel class of KDR kinase inhibitors. *Bioorg. Med. Chem. Lett.* **2003**, *13*, 1673−1677. (b) Bardelle, C.; Cross, D.; Davenport, S.; Kettle, J. G.; Ko, E. J.; Leach, A. D.; Mortlock, A.; Read, J.; Roberts, N. J.; Robins, P.; Williams, E. J. Inhibitors of the tyrosine kinase EphB4. Part 1: structure-based design and optimization of a series of 2,4-bis-anilinopyrimidines. *Bioorg. Med. Chem. Lett.* **2008**, *18*, 2776−2780.

(16) Force, T.; Krause, D. S.; Van Etten, R. A. Molecular mechanisms of cardiotoxicity of tyrosine kinase inhibition. *Nat. Rev. Cancer* **2007**, *7*, 332−344.

(17) Lawhorn, B. G.; Philp, J.; Graves, A. P.; Holt, D. A.; Gatto, G. J., Jr.; Kallander, L. S. Substituent effects on drug-receptor H-bond interactions: correlations useful for the design of kinase inhibitors. *J. Med. Chem.* **2016**, *59*, 10629−10641.

(18) (a) Ertl, P.; Rohde, B.; Selzer, P. Fast calculation of molecular polar surface area as a sum of fragment-based contributions and its application to the prediction of drug transport properties. *J. Med. Chem.* **2000**, *43*, 3714−3717. (b) Palm, K.; Stenberg, P.; Luthman, K.; Artursson, P. Polar molecular surface properties predict the intestinal absorption of drugs in humans. *Pharm. Res.* **1997**, *14*, 568−571. (c) Kelder, J.; Grootenhuis, D. J.; Bayada, D. M.; Delbressine, L. P. C.; Ploemen, J.-P. Polar molecular surface as a dominating determinant for oral absorption and brain penetration of drugs. *Pharm. Res.* **1999**, *16*, 1514−1519.

(19) (a) Harris, L. S.; Zhang, S.; Treskov, I.; Kovacs, A.; Weinheimer, C.; Muslin, A. J. Raf-1 kinase is required for cardiac hypertrophy and cardiomyocyte survival in response to pressure overload. *Circulation* **2004**, *110*, 718−723. (b) Muslin, A. J. Role of Raf proteins in cardiac

hypertrophy and cardiomyocyte survival. *Trends Cardiovasc. Med.* **2005**, *15*, 225−229.

(20) Lawhorn, B. G.; Philp, J.; Graves, A. P.; Shewchuk, L.; Holt, D. A.; Gatto, G. J., Jr.; Kallander, L. S. GSK114: a selective inhibitor for identifying the biological role of TNNI3K. *Bioorg. Med. Chem. Lett.* **2016**, *26*, 3355−3358.

(21) The calculated TPSA (143 Å$^2$) of the 4-sulfone analogs exceeds the limit required for oral bioavailability within the series. However, these analogs were expected to retain oral bioavailability (as observed) based on their presumed internal H-bond with the neighboring aniline NH, which is unaccounted for in the TPSA calculation, leading to an overestimated value of PSA.

(22) (a) Hammond, M.; Kallander, L. S.; Lawhorn, B. G.; Philp, J.; Sarpong, M. A.; Seefeld, M. A. Azolopyrimidine Compounds as Kinase Inhibitors and Their Preparations and Use in the Treatment of Diseases and Methods. PCT Int. Appl. WO2011149827, 2011. (b) Kallander, L. S.; Lawhorn, B. G.; Philp, J.; Zhao, Y. 3-[(6-Aminopyrimidin-4-yl)amino]benzenesulfonamide Compounds Useful as TNNI3K Inhibitors, Their Preparation, and Methods of Use in the Treatment of Congestive Heart Failure. PCT Int. Appl. WO2011088027, 2011. (c) Kallander, L. S.; Philp, J. Compounds for Treating Congestive Heart Failure. PCT Int. Appl. WO2011088031, 2011.

(23) Hartung, C. G.; Backes, A. C.; Felber, B.; Missio, A.; Philipp, A. Efficient microwave-assisted synthesis of highly functionalized pyrimidine derivatives. *Tetrahedron* **2006**, *62*, 10055−10064.